Preliminary $^{40}Ar/^{39}Ar$ geochronology of igneous intrusions from Uvalde County, Texas: Defining a more precise eruption history for the southern Balcones Volcanic Province

By Daniel P. Miggins, Charles D. Blome, and David V. Smith

U.S. Geological Survey Open-File Report 2004-1031

U.S. DEPARTMENT OF THE INTERIOR
U.S. GEOLOGICAL SURVEY

Table of Contents

Introduction

Volcanic and subvolcanic intrusive rocks in south-central Texas have been known since the earliest geological surveys of Texas (Lonsdale, 1927 and Sayre,1936). In addition to their geologic setting, the rocks provide a unique economic resource for the state of Texas (road aggregate and natural gas). The first subsurface occurrences of these Cretaceous rocks were reported in the 1920Õs, and by the 1950Õs numerous gas fields were discovered in Zavala and Dimmit counties.

The Uvalde igneous field consists of fine to coarse-grained ultramafic and hypabyssal rocks that occur as dikes, plugs, and shallow intrusions. Olivine, clinopyroxene, and feldspathoids constitute 25-60% of the exposed rocks. There are five rock types within the Uvalde igneous field: alkali basalt, melilite-olivine nephelinite, olivine nephelinite, nepheline basanite, and phonolite. The field is centered in Uvalde County and extends to the west into Kinney County (Figure 1) and to the east as far as Bexar County. Isolated dikes and plugs also occur 240 km to the northeast in Hill County near Austin, Texas.

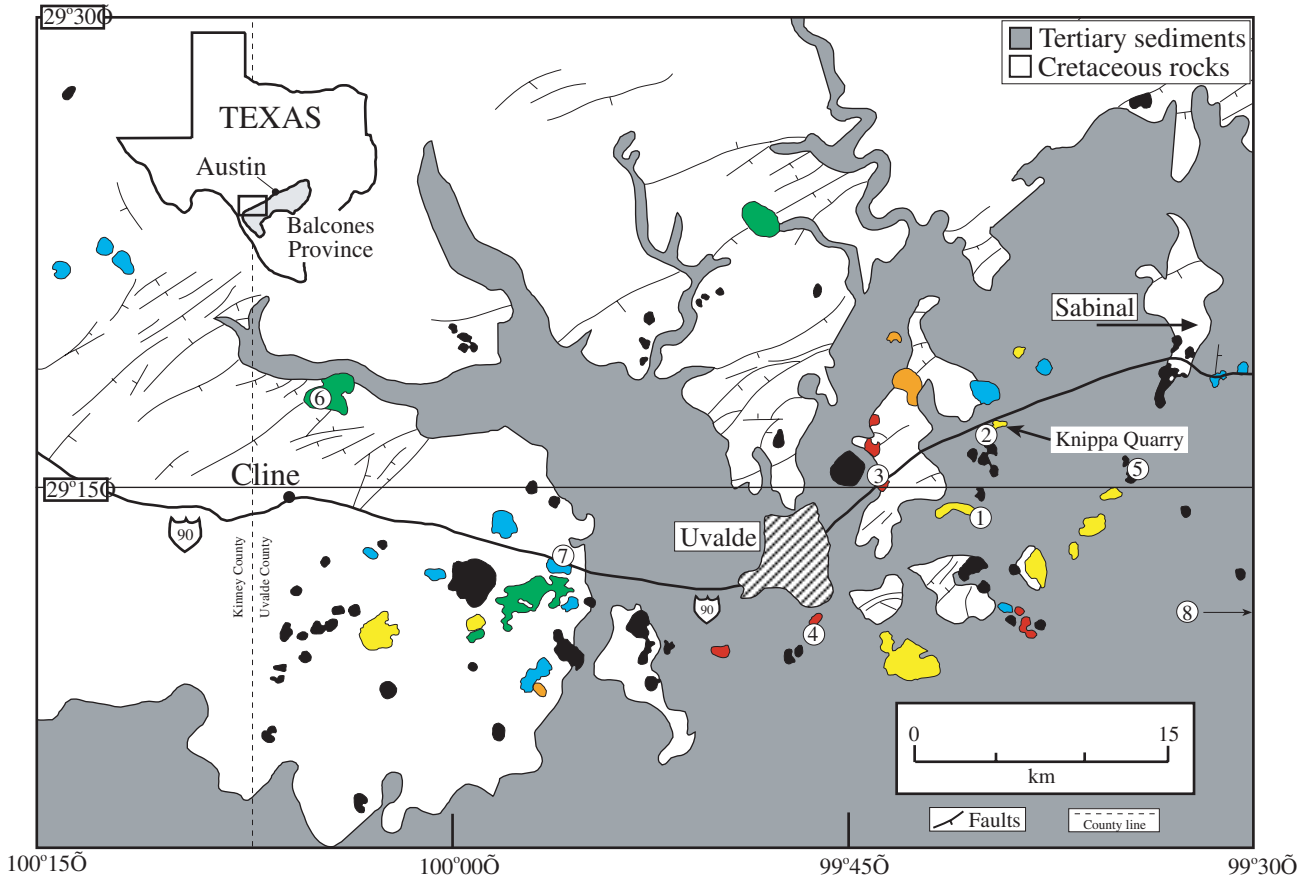

Figure 1. The Uvalde area of the Balcones magmatic province modified from Wittke and Lawrence, 1993 (after Barnes, 1974, 1977). Note. Sample 01-CB-010 is off the map approximately 5 km south of Sabinal.

The intrusive rocks in Uvalde County are economically important; formed natural gas traps by intense folding and faulting as they intruded surrounding Late Cretaceous sedimentary rocks (Figure 1). The igneous rocks also act as barriers to groundwater flow. The vesicles in the rocks are by filling with secondary minerals, thereby decreasing permeability of the igneous rocks. The Uvalde igneous field may also influence the major Edwards aquifer flow paths where there is a markedly change in direction just east of the Uvalde intrusions (Maclay, 1995).

A high-resolution aeromagnetic survey flown in 2001 (Smith and others, 2002) detected over 200 shallow igneous intrusive bodies, where fewer than 30 have surface expression. The aeromagnetic map, shown in Figure 2a, reveals numerous small bump-like magnetic anomalies in the southwest quadrant. These anomalies are set against broader regional magnetic highs (red) and lows (blue). Igneous rocks contain much more magnetite than limestone, thus the contrast in magnetic susceptibilities causes distinct distortions in the earthÕs magnetic field at the surface. These anomalies effectively distinguish the intrusive rocks from the surrounding country rock. Using matched-filtering techniques on the aeromagnetic data, the shallow (0 Ð 500 m) anomalies were separated from those due to moderately deep plutons and crystalline basement. A map of inferred igneous outcrops and subcrops, set against a regional geologic map, is shown in Figure 2b.

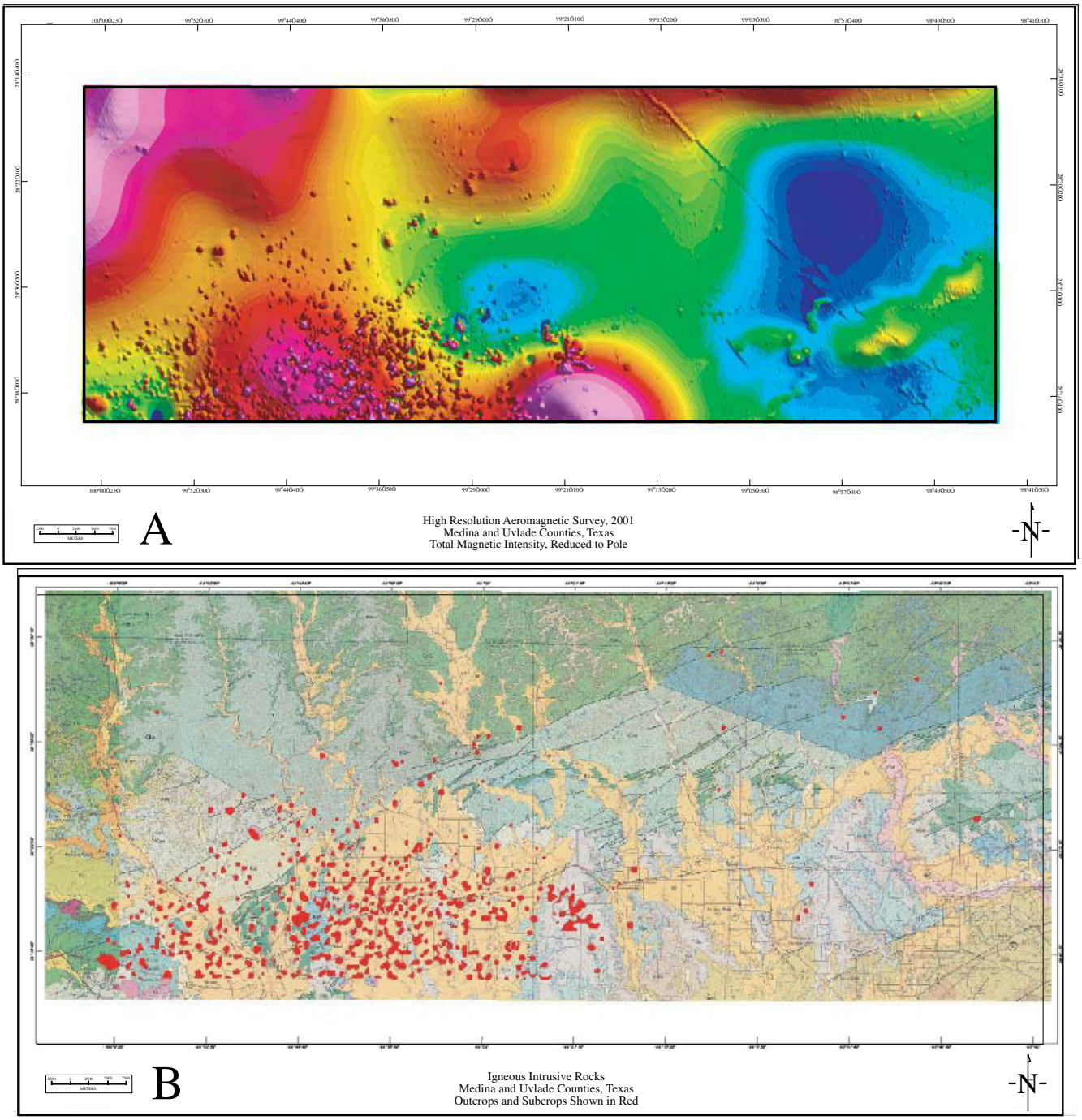

Figure 2. Aeromagnetic map (2a) and map of inferred igneous outcrops and subcrops, set against a regional geologic map (2b).

The apparent random distribution of these igneous bodies, and the sparcity of associated dikes or dike-like structures, raises the question of their origins in time, as to whether they represent a single intrusive episode or several. This question can best be answered by isotopic, geochemical, and geochronological analysis. This report contains preliminary $^{40}Ar/^{39}Ar$ geochronology of various mineral separates, as well as groundmass concentrates, from a variety of rock types exposed within Uvalde County. Previous K/Ar age constraints reported by Baldwin and Adams (1971) indicate that igneous activity spanned a range in age from 90 to 60 Ma. Due to the inherent problems associated with the K-Ar dating technique, especially on basaltic rocks, the overall goal of this work is to define a more precise emplacement history of these igneous rocks. The $^{40}Ar/^{39}Ar$ ages obtained for the Uvalde rocks yield two distinct groups of ages, one at approximately 82-20 Ma and the other at 74-72 Ma.

Methodology

Mineral separates were analyzed using the $^{40}Ar/^{39}Ar$ age spectrum technique, a variant of the conventional K/Ar method. A mineral separate of unknown age and a mineral standard of known age (Fish Canyon Tuff [FCT] sanidine with an age of 28.03 Ma) were irradiated at the USGS TRIGA reactor in Denver, Colorado, following techniques described by Dalrymple et al., (1981) to produce ^{39}Ar from ^{39}K by neutron bombardment. After irradiation, the ^{40}Ar radiogenic/^{39}Ar potassium ratios of the sample and standard were determined. Standard techniques were employed to produce $^{40}Ar/^{39}Ar$ spectra as described by Snee (1982), Snee et al., (1988), and Snee, (2002).

The isotopic composition of argon was measured at the USGS in Denver, Colorado using a MAP 215 series rare-gas mass spectrometer made by Mass Analyzer Products Limited. Abundances of five argon isotopes (^{40}Ar, ^{39}Ar, ^{38}Ar, ^{37}Ar, and ^{36}Ar) were measured in each sample. Argon was released from the samples in 7 to 11 temperature steps. Radiogenic ^{40}Ar ($^{40}Ar_R$) is the total ^{40}Ar derived from natural radioactive decay of ^{40}K after all corrections from non-decay-derived ^{40}Ar, including atmospheric ^{40}Ar and reactor-produced ^{40}Ar, have been made. Potassium-derived ^{39}Ar (^{39}ArK) is the total ^{39}Ar derived from the epithermal neutron-induced $^{39}K(n, p)$ ^{39}Ar after corrections for non-^{39}K-derived ^{39}Ar, including ^{42}Ca-derived ^{39}Ar, are made. F is the quantity resulting from the division of radiogenic ^{40}Ar and K-derived ^{39}Ar. Quantities for radiogenic ^{40}Ar and K-derived ^{39}Ar are given in volts of signal measured on a Faraday detector by a digital voltmeter. These quantities can be converted to moles using the mass spectrometer sensitivity at time of measurement of 9.736x10-13 moles of argon per volt of signal. The measured $^{40}Ar/^{39}Ar$ ratio used for mass descrimination correction is 298.9.

Samples were irradiated in two irradiation packages (DD78, DD79) for times ranging from 20 to 40 hours at 1 megawatt in the USGS TRIGA reactor in Denver. The J-value for each sample was determined from adjacent standards; errors in the calculated J-value were determined experimentally by calculating the reproducibility of multiple monitors. Corrections for the irradiation-produced, interfering isotopes of argon were made by measuring the production ratios for the interfering isotopes of argon produced in pure salts of K_2SO_4 and CaF_2 irradiated simultaneously with the samples of this study.

Corrections were made for additional interfering isotopes of argon produced from irradiation of chlorine using the method described by Roddick (1983). Measured quantities of ^{37}Ar and ^{39}Ar were corrected for radioactive decay, and the $^{39}Ar/^{37}Ar$ ratios were corrected for this decay, as well as for interfering argon isotopes. By multiplying the $^{39}Ar/^{37}Ar$ ratios by 0.5, the relative approximate K/Ca distribution of the samples may be obtained. Error estimates for apparent ages of individual temperature steps were assigned by using the equations of Dalrymple et al., (1981). However, the equations were modified to allow the option of choosing the larger of separately derived errors in the F-value-either a calculated error or an experimental error determined from the reproducibility of identical samples. Age plateaus were determined by comparing contiguous gas fractions using the critical value test of Dalrymple and Lanphere (1969), and McIntyre (1963), and the error was determined using the equations of Dalrymple et al., (1981). Isochron analysis (York, 1969) for those samples that did not plateau was used to assess if nonatmospheric argon components were trapped in any samples and in some cases to define an apparent age of the sample.

Sample Preparation

Mineral separates of potassium feldspar (K-feldspar) and plagioclase, as well as groundmass concentrates were used in this study. High-purity mineral separates (>99%) of K-feldspar, as well as basalt groundmass concentrates (>95-98% purity), were obtained using standard separation techniques. Mineral concentrates were selected by choosing the largest size-range free of composite grains and were purified using magnetic and heavy-liquid techniques. Final mineral separates were hand picked under a binocular microscope to a purity of >99%, with particular attention being paid to excluding grains with abundant inclusions, adhering material, carbonate, or alteration. All mineral separates and groundmass concentrations were treated in a dilute bath of HCl (<10%) for 15-30 minutes to dissolve any primary and secondary calcite and zeolites. K-feldspar separates were treated in a dilute bath of HF (~15%) for approximately 5-15 minutes, depending on the purity of the crystals, to remove glass, zeolites and other material adhering to the crystals.

All groundmass concentrates range in size from 46 to 100 mesh (180-150 mm). Visible phenocrysts of olivine, pyroxene, and feldspathoids were removed from the concentrate using a magnetic separator. Both mineral and groundmass concentrates were washed in acetone, alcohol, and deionized water (2X) to dissolve any organic residue and remove dust.

Results

Eight samples were collected and 11 $^{40}Ar/^{39}Ar$ ages were obtained from K-feldspar, plagioclase and groundmass concentrates. Table 1 lists the interpreted ages for each sample, latitude and longitude of the collection site, and their location relative to the town of Uvalde. Replicate analyses for samples 01-CB-002 and 01-CB-005 were done to check sample reproducibility. Plagioclase and a groundmass concentrate were analyzed for sample 01-CB-008 to test the reproducibility of both mineral phases from the same rock. All age spectra and the justification for interpreted ages are described below.

A groundmass concentrate for sample 01-CB-001A (Figures 1 and 3) comes from an outcrop along the banks of the Frio River. The age spectrum for this sample is disturbed exhibiting much older apparent ages in the middle temperature-release steps. The age spectrum shows that the argon system of this sample has been severely affected over geologic time. No interpretable age can be deduced.

Table 1. Summary of sample data along with location and ages for the intrusions from Uvalde County, Texas

Sample	# on Fig 1	Location	Min/GC	Latitude	Longitude	Type of date Apparent	Age (Ma)	Initial $^{40}Ar/^{36}Ar$
01-CB-001A	1	Intrusion along Frio River	GC	29°14'10"	99°40'58"		NA	
01-CB-002	2	Knippa quarry - Run #1 (82-100 mesh)	GC	29°17'12"	99°39'25"	Total-gas age Isochron age (steps 1-7)	80.9 ± 0.6 76 ± 7	241 ± 39
		Run #2 (46-60 mesh)	GC			Average age (steps 4-6) Isochron age (steps 1-8)	80.48 ± 0.29 82.7 ± 2	287 ± 16
01-CB-005	3	Intrusion on highway 90 east of Uvalde - Run #1	K-feldspar	29°15.338'	99°43.842'	Average age (steps 5-6) Isochron age (steps 2-6)	72.41 ± 0.15 71.5 ± 1.1	423 ± 57
		Run #2	K-feldspar			Average age (steps 4-7) Isochron age (steps 1-7)	72.60 ± 0.26 74.1 ± 1.0	268 ± 8
01-CB-006	4	Intrusion at Fort Inge south of Uvalde	K-feldspar	29°10.841'	99°45.936'	Average age (steps 9-11) Isochron age (steps 1-11)	73.39 ± 0.13 74.6 ± 1.2	336 ± 226
01-CB-007	5	Intrusion southest of Uvalde	GC	29°15.576'	99°34.723'	Maximum age (step 7) Isochron age (steps 1-9)	79.2 ± 0.6 105 ± 27	287 ± 67
01-CB-008	6	Intrusion north of Cline	Plagioclase	29°17.813'	100°04.884'	Average age (steps 3-7) Isochron age (steps 2-8)	80.92 ± 0.16 80.36 ± 0.91	300 ± 33
			GC			Minimum age (step 5) Isochron age (steps 3-6, 8)	82.79 ± 0.13 82.68 ± 0.24	252 ± 7
01-CB-009	7	Intrusion on highway 90 west of Uvalde	GC	29°12.869'	99°55.911'	Weight average (steps 2-7) Isochron age (steps 1-8)	78.9 ± 1.4 74.0 ± 7	188 ± 7
01-CB-010	8	Intrusion south of Sabinal at Pilot Knob Hill	GC	29°11'38"	99°25'12"	Maximum age (Step # 3) Isochron age (steps 1-9)	78.52 ± 0.12 80.0 ± 7	281 ± 23

G.C.- Groundmass Concentrate
MIN - Mineral
NA - No Age

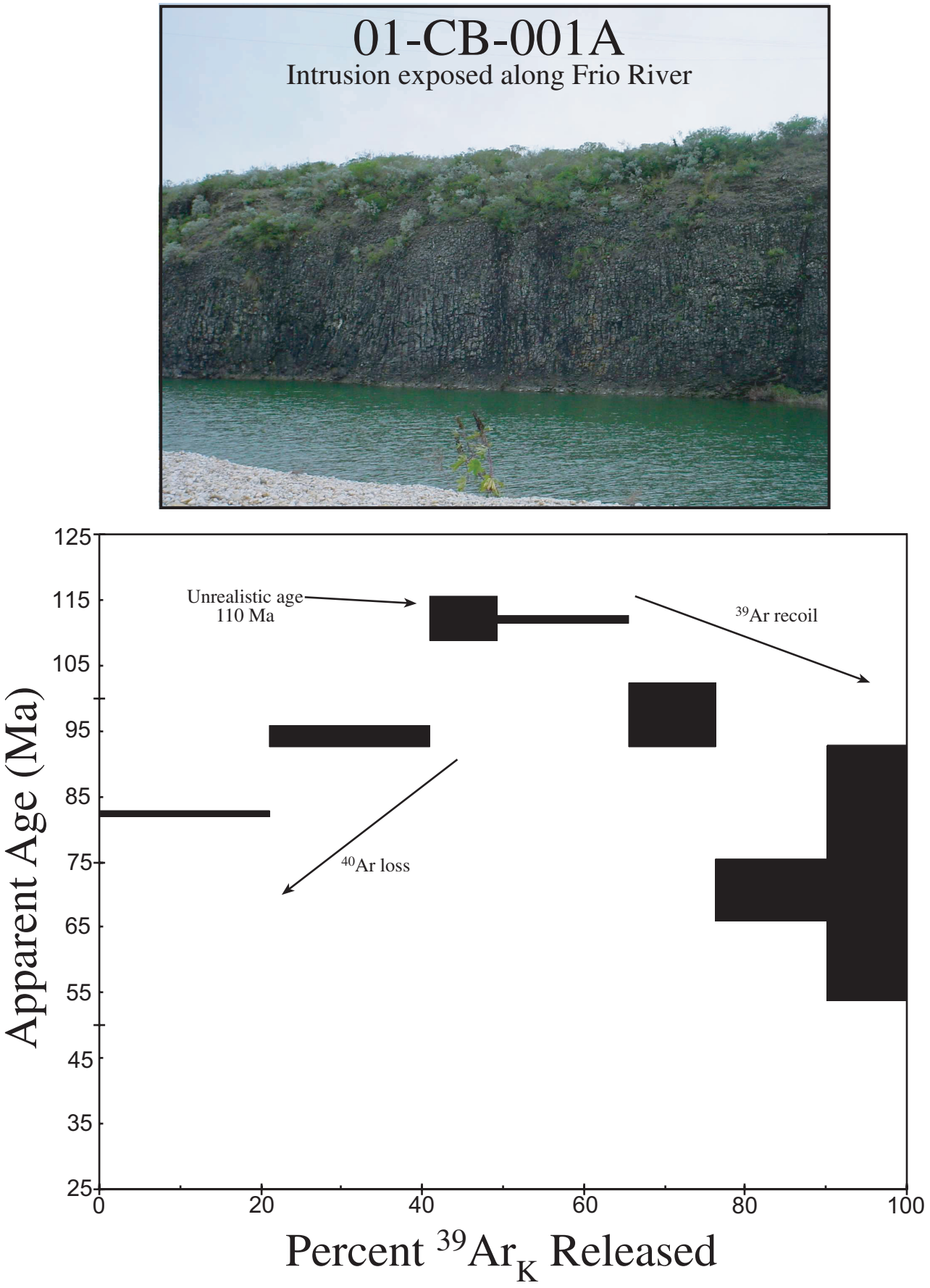

Figure 3. Age spectrum and photograph for sample 01-CB-001A.

Sample 01-CB-002, a melilite-olivine nephelinite, was collected from Knippa Quarry. This quarry is currently being mined for road aggregate (Figures 1 and 4). Two fractions of groundmass concentrate were prepared. The first sample was sieved to a final mesh size of 82-100 mesh. The age spectrum for this finer-grained fraction shows the effects of ^{39}Ar recoil. Assuming that the recoiled ^{39}Ar was distributed within the sample and not lost from the sample, and assuming the sample had not lost radiogenic ^{40}Ar over time, the total-gas age for this sample would be the best estimate of its emplacement age. The total-gas age is 80.9±0.6 Ma. An isochron for this sample gave an age of 76±7 Ma. The large error reflects the relatively poor fit of the data to a single 2-component mixing line; thus the total-gas age is likely disturbed. The argon analysis for the 46-60 mesh size fraction yielded a less discordant age spectrum, but likely exhibits the effects of excess argon. The age given for this second sample is 80.48±0.29 Ma and an isochron age that is slightly older, although within error, at 82±2 Ma. The smaller error of the isochron age provides more confidence in the geologic meaning of the age.

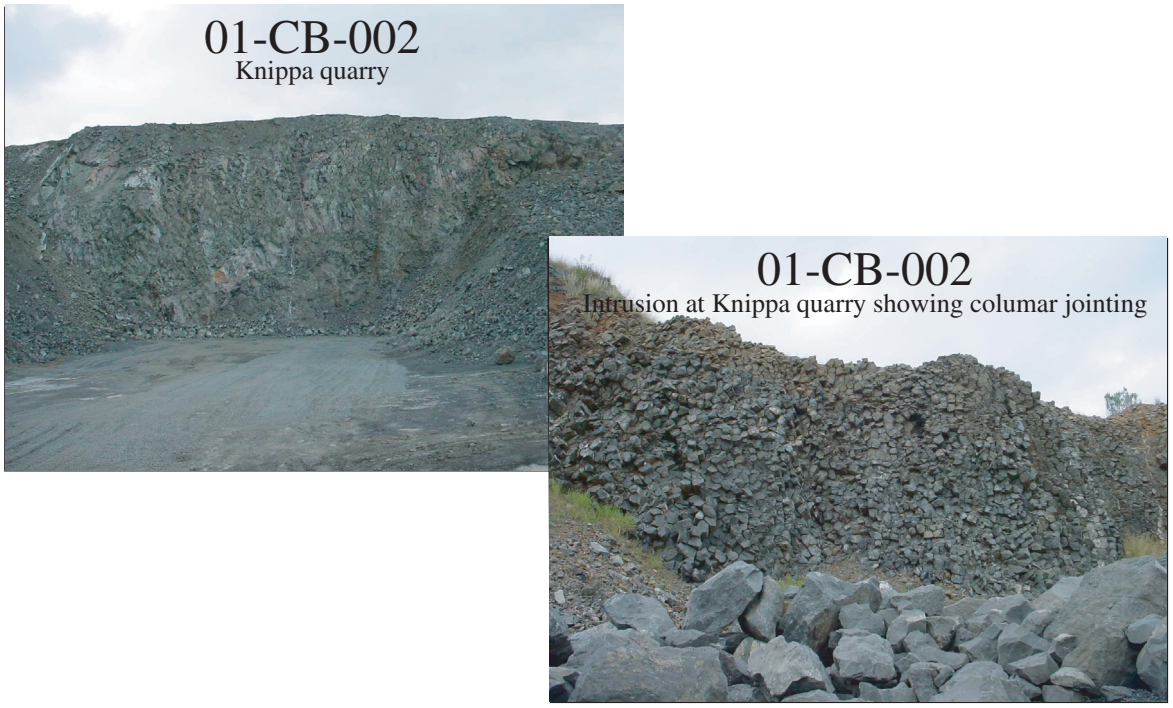

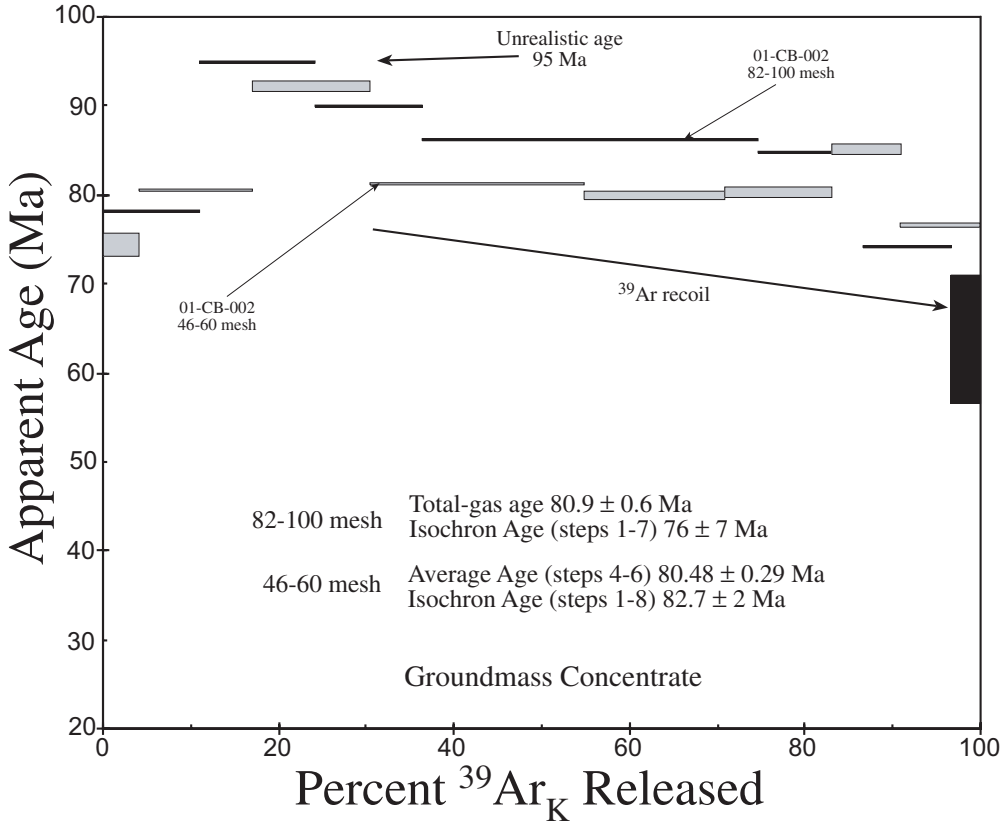

Figure 4. Age spectrum and photographs of sample 01-CB-002 at Knippa Quarry.

Sample 01-CB-005 is from a phonolite that is poorly exposed along highway 90 west of Uvalde (Figures 1 and 5). Two fractions of K-feldspar from sample 01-CB-005 were analyzed. Both age spectra are disturbed, and the disturbance may be a result of excess argon or ^{39}Ar recoil. Both K-feldspar fractions yielded average ages of 72.41±0.15 Ma and 72.60±0.26 Ma with corresponding isochron ages of 71.5±1.1 Ma and 74.1±1.0 Ma, respectively. Another phonolite rock (01-CB-006) was collected at Fort Inge, south of Uvalde (Figures 1 and 6). The K-feldspar separated from this sample yielded an average age of 73.39±0.13 Ma. An isochron for this sample yielded an age of 74.6±1.2 Ma. This sample also contained excess argon in the lower temperature release steps, but not as significant a component as in sample 01-CB-005.

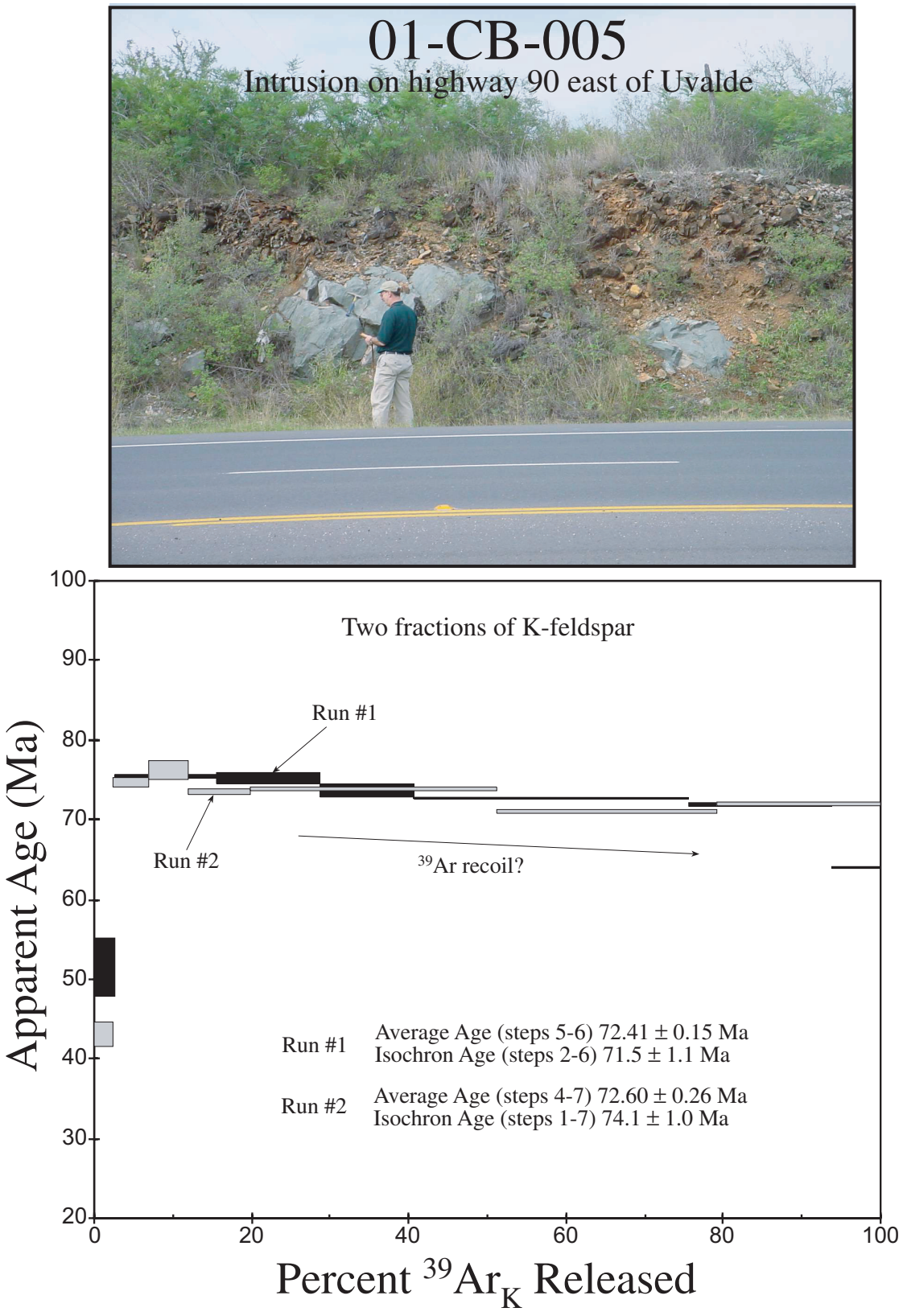

Figure 5. Age spectrum and photograph of sample 01-CB-005 on highway 90 east of Uvalde.

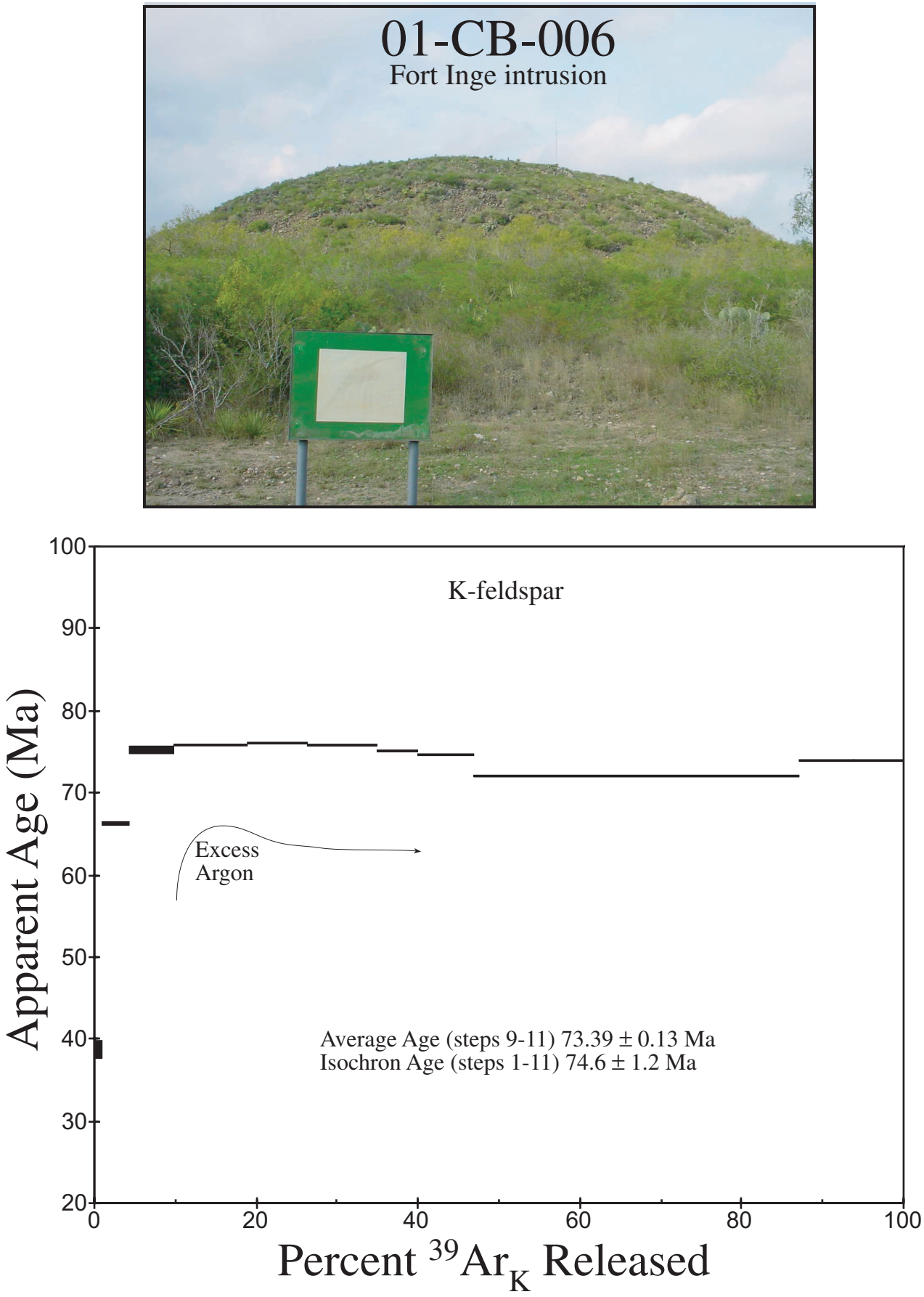

Figure 6. Age spectrum and photograph of sample 01-CB-006 south of Uvalde.

Sample 01-CB-007 was collected from a gentle sloping mound mostly covered by vegetation southeast of Uvalde (Figures 1 and 7). A groundmass concentrate yielded a very discordant age spectrum. At heating step #3, the age is 150 Ma (Figure 7). This high apparent age is likely the result of the incorporation of large amounts of excess argon in the sample. However, step #7 is the lowest point in the saddle and gives an age of 79.17±0.56 Ma, the maximum possible age for this sample. The isochron for this sample gives an age of approximately 105 Ma, again an unrealistic age for this intrusion.

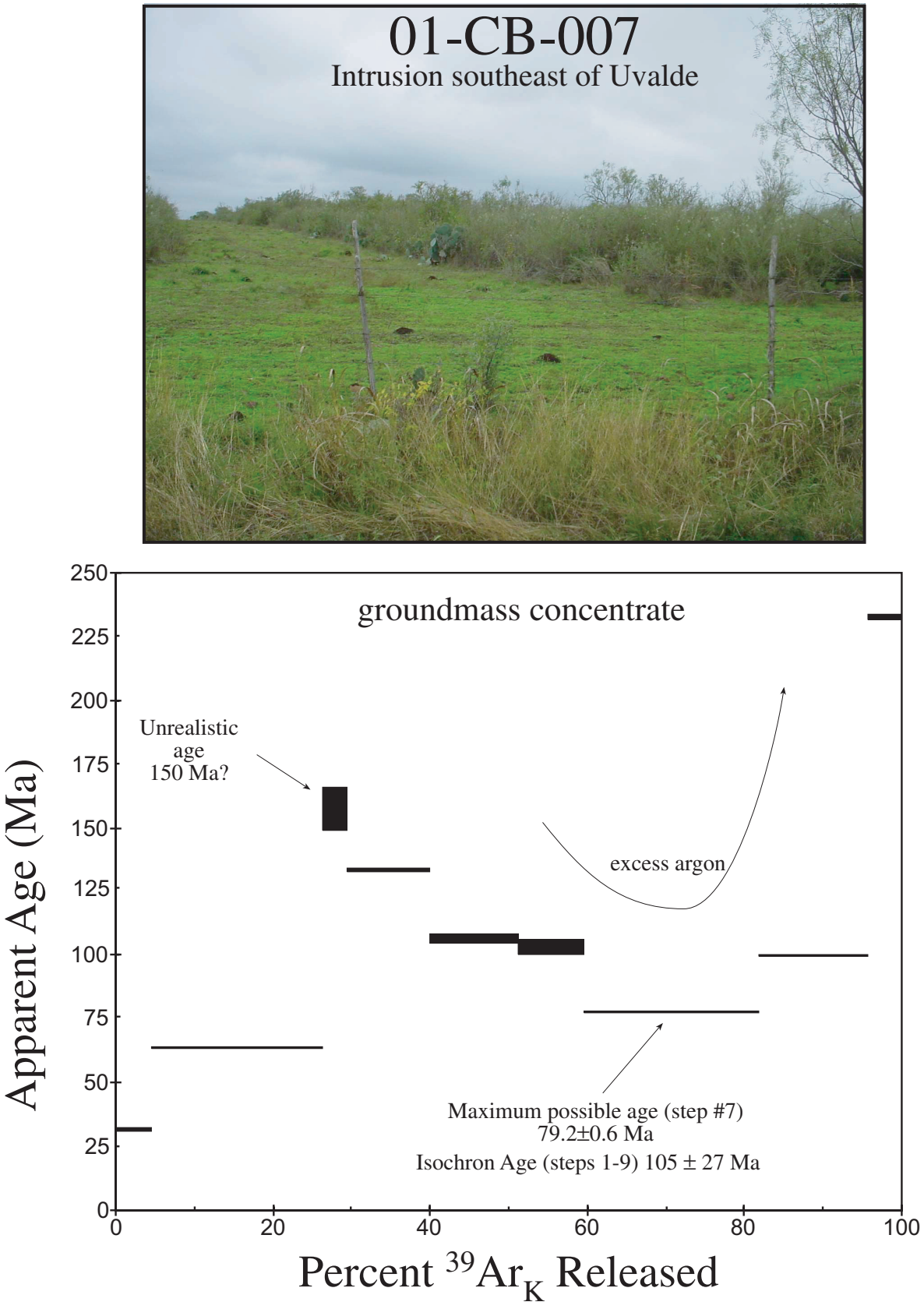

Figure 7. Age spectrum and photograph of sample 01-CB-007 southest of Uvalde.

A basalt (01-CB-008) from an area north of Cline (west of Uvalde) is the westernmost rock analyzed (Figures 1 and 8). For this sample a concentrate of plagioclase and a groundmass concentrate were prepared. An average age of 80.92±0.16 Ma for the plagioclase and 82.79±0.13 Ma for heating step #5 for the groundmass concentrate are given for these samples. Their associated isochron ages are 80.36±0.91 Ma and 82.68±0.24 Ma, respectively. Both the plagioclase and the groundmass concentrate showed significant 40Ar loss in the lower temperature heating steps.

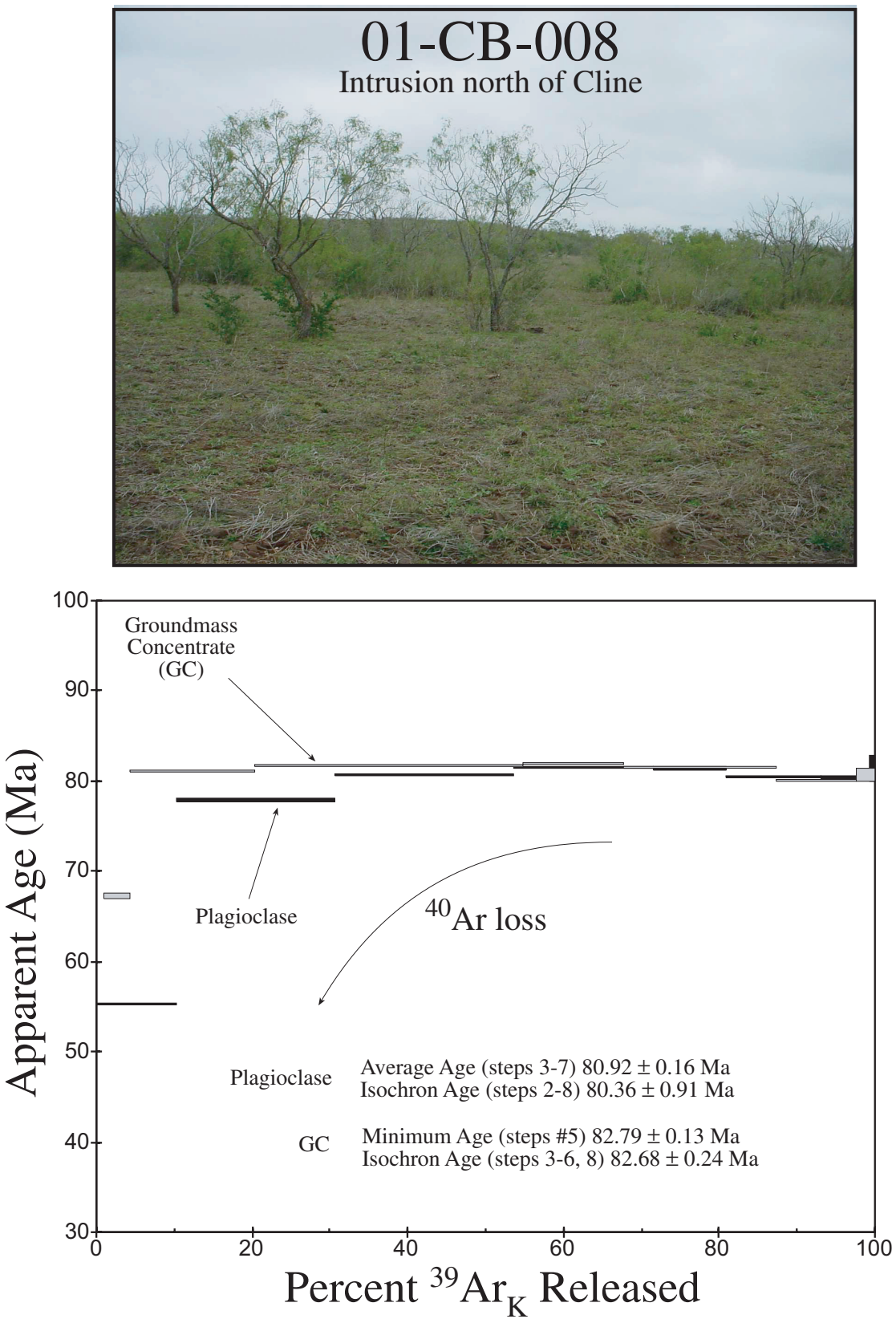

Figure 8. Age spectrum and photograph of sample 01-CB-008 north of Cline.

Sample 01-CB-009 was collected off of highway 90 west of Uvalde southeast of sample 01-CB-008. Again, like most of the groundmass concentrates in this study, a groundmass concentrate for this sample yielded abundant ^{39}Ar recoil (Figures 1 and 9). The age spectrum is very discordant, but a weight average of steps 2 to 7 gives an age of 78.2±1.4 Ma. This weight average age is within error of the isochron age of 74.0±7 Ma.

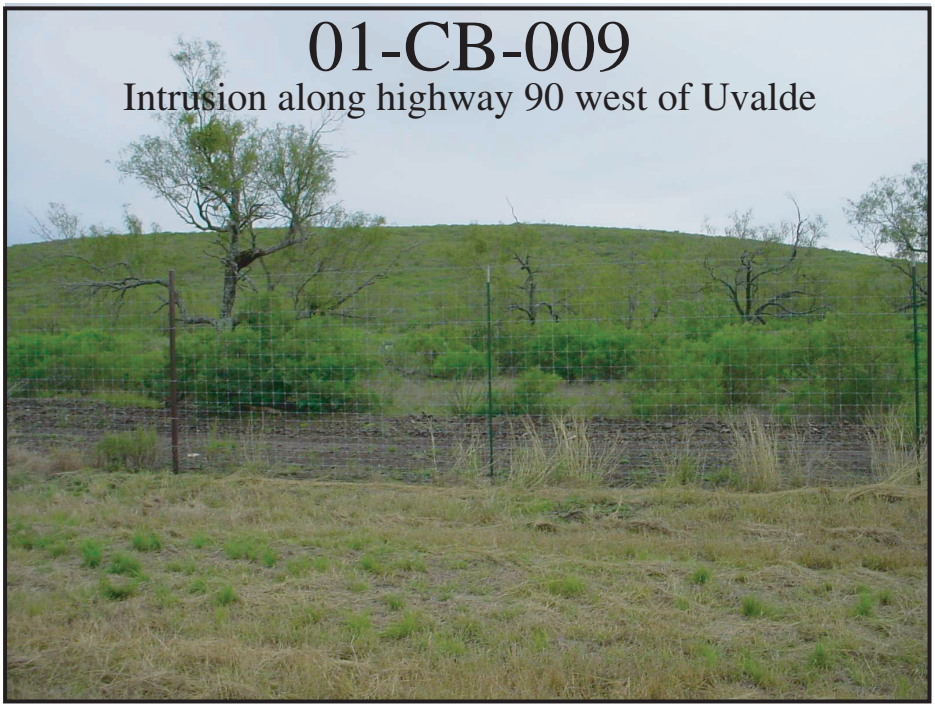

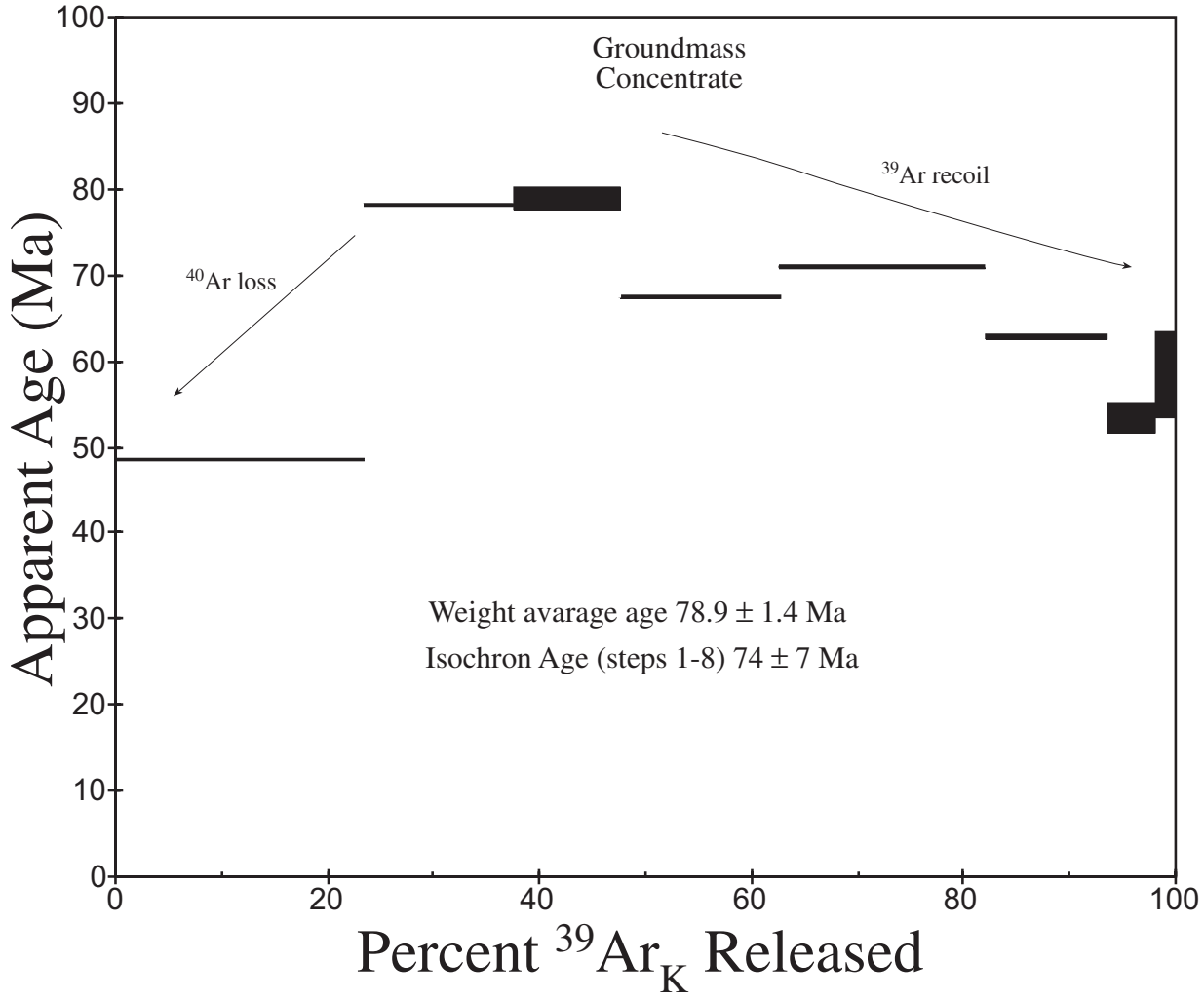

Figure 9. Age spectrum and photograph of sample 01-CB-09 on highway 90 west of Uvalde.

Sample 01-CB-010 was collected from Pilot Knob Hill, located south of Sabinal (Figures 1 and 10). A groundmass concentrate for this sample yielded an age spectrum that may reflect either excess argon or ^{39}Ar recoil in the lower temperature steps. However, 64.9% of the gas was released in the 1400oC heating step and most likely represents the closest possible age for this intrusion at 78.52±0.12 Ma. The isochron age for this sample is 80±8 Ma.

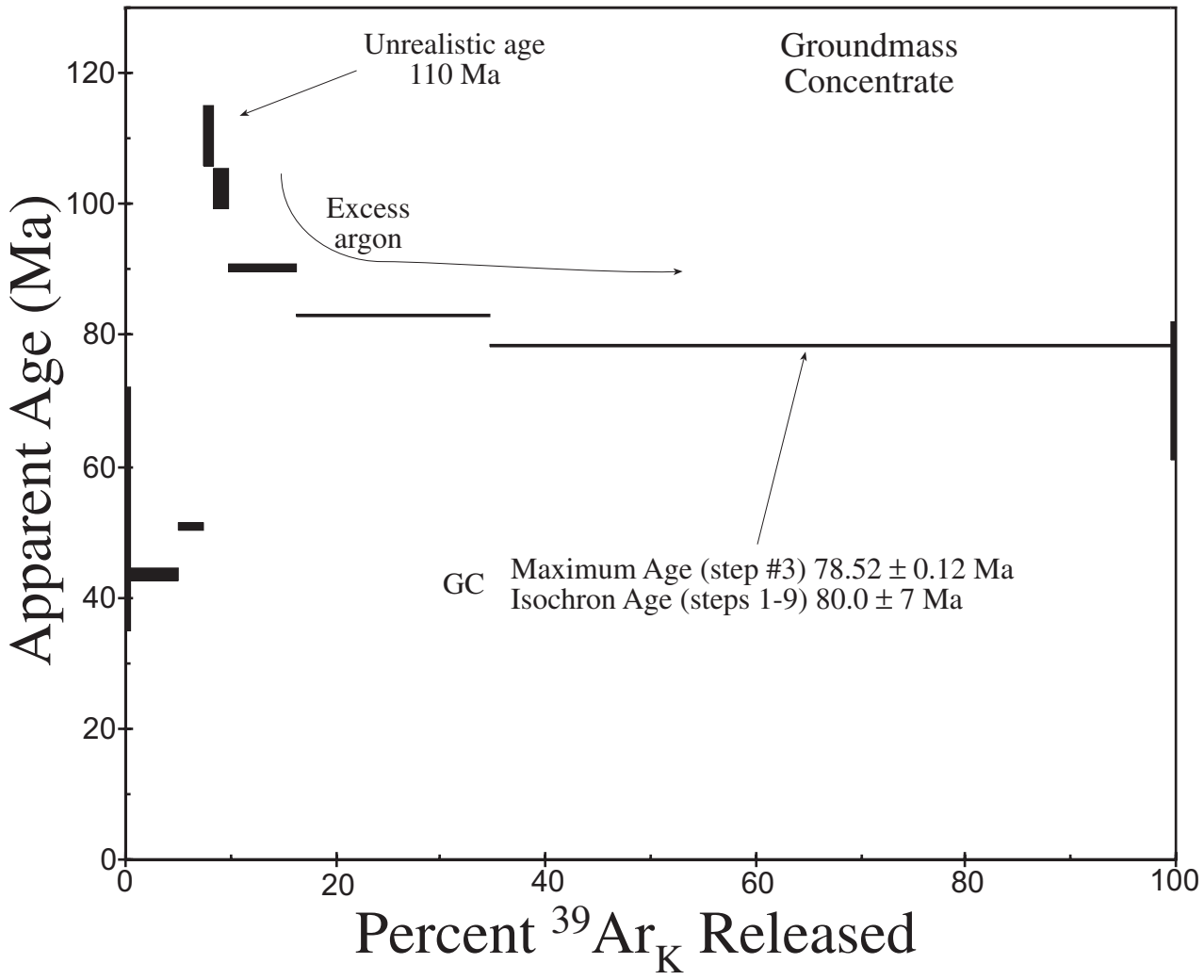

Figure 10. Age spectrum for sample 01-CB-010 on highway 90 west of Uvalde.

Conclusions

Step-heating on minerals and groundmass concentrates for these rocks all yielded discordant age spectra and as a result, determining emplacement ages is difficult at best. However, confidence in the interpretation of complex age spectra from groundmass concentrates and mineral separates has been documented for igneous rocks associated with the northern Rio Grande Rift (Miggins, 2002 and Miggins et al., 2002). Moreover, there is a high degree of confidence in the ages for the K-feldspar samples from 01-CB-005 and 01-CB-006, as well as for the plagioclase and groundmass concentrate from sample 01-CB-008. By comparing the other samples to samples 01-CB-005, 01-CB-006, and 01-CB-008 with a high degree of confidence in their crystallization age, two distinct emplacement ages have emerged from the $^{40}Ar/^{39}Ar$ data.

The age spectra indicate that there are two distinct phases of magmatic activity in the southwestern Balcones igneous zone. The first phase of intrusions was emplaced approximately 82-80 m.y. ago. The younger phase of intrusions, the phonolites, was emplaced approximately 74-72 m.y. ago.

Future Work

Future studies for the Uvalde rocks will include the dating of nepheline. Alunite from hydrothermal mineralization associated with the intrusions will be analyzed to determine if the formation of alunite occurred during or after the emplacement of the intrusions. Also, samples will be collected from the southernmost, westernmost, and northernmost exposures to determine if there is a geographic spread in the ages of the intrusions based on geochronological, geochemical, and isotopic data.

Acknowledgments

The authors wish to thank Ross Yeoman and Libby Prueher for their assistance in analyzing the samples and Jason Faith for helping to collect samples for this study. Reviews by Mel Kuntz and Larry Snee greatly improved the clarity of this report.

References Cited

Baldwin O.D., and Adams, J.A.S., 1971, K^{40}/Ar^{40} ages of the alkalic igneous rocks of the Balcones Fault Trend of Texas, The Texas Journal of Science, v. 22, no. 2&3, pp 223-231.

Barnes, V.E., 1974, San Antonio Sheet, Geologic Atlas of Texas: Bureau of Econonic Geology, University of Texas, scale 1: 250,000.

Barnes, V.E., 1977, Del Rio Sheet, Geologic Atlas of Texas: Bureau of Econonic Geology, University of Texas, scale 1: 250,000.

Dalrymple, G.B., and Lanphere, M.A., 1969, Potassium-argon dating: Principles, techniques, and applications to geochronology: W.H. Freeman and Company, San Francisco, 258 pp.

Dalrymple, G.B., Alexander, E.C., Lanphere, M.A., and Kraker, G.P., 1981, Irradiation of samples for $^{40}Ar/^{39}Ar$ dating using the Geological Survey TRIGA reactor: U.S. Geological Survey Professional Paper 1176, 55 p.

Lonsdale, J.T., 1927, Igneous rocks of the Balcones fault region of Texas: University of Texas Bulletin 2744, 178 p.

Maclay, R.W., 1995, Geology and hydrology of the Edwards Aquifer in the San Antonio area, Texas: Water-resources Investigations Report 95-4186, U.S. Geological Survey.

McIntyre, D.B., 1963, Precision and resolution in geochronometry: in Albritton, C.C., ed., The fabric of geology, Addison-Wesley, Reading, Massachusetts, p. 112-134.

Miggins, D.P., 2002, Chronologic, geochemical, and isotopic framework of igneous rocks within the Raton Basin and adjacent Rio Grande Rift, south-central Colorado and northern New Mexico, Univ. of Colorado, Boulder, Colorado, 417p.

Miggins, D.P., Thompson, R.A., Pillmore, C.L., Snee, L.W., and Stern, C.R., 2002, Extension and uplift of the northern Rio Grande Rift: Evidence from $^{40}Ar/^{39}Ar$ geochronology from the Sangre de Cristo Mountains, south-central Colorado and northern New Mexico, in Menzies, M.A., Klemperer, S.L., Ebinger, C.J., and Baker, J., eds., Volcanic Rifted Margins: Boulder Colorado, Geological Society of America Special Paper 362, p. 47-64.

Roddick, J.C., 1983, Generalized numerical error analysis with applications to geochronology and thermodynamics: Geochimica et Cosmochimica Acta, v. 51, p. 2129-2135.

Sayre, A.N., 1936, Geology and groundwater resources of Uvalde and Medina Counties, Texas: U.S. Geological Survey Water-Supply Paper 678, 146 p.

Smith, D.V., Smith, B.D., Hill, P.L., 2002, Aeromagnetic survey of Medina and Uvalde Counties, Texas: Open-File Report 02-49, U.S. Geological Survey.

Snee, L.W.,1982, Emplacement and cooling of the Pioneer Batholith, south-western Montana: Columbus, Ohio, The Ohio State University Ph.D. dissertation, 320 p.

Snee, L.W., 2002, Argon thermochronology of mineral depositsÑa review of analytical methods, formulations, and selected applications: U.S. Geological Survey Bulletin 2194, 44 p.

Snee, L.W., Sutter, J.F., and Kelly, W.C., 1988, Thermochronology of economic mineral deposits: Dating the stages of mineralization at Panasqueira, Portugal, by high-precision $^{40}Ar/^{39}Ar$ age-spectrum techniques on muscovite: Economic Geology, v. 83, 335-354.

Wittke, J.H., and Lawrence, L.E.,1993, OIB-like mantle source for continental alkaline rocks of the Balcones Province, Texas: trace-element and isotopic evidence, The Journal of Geology, v. 101, pp. 333-344.

York, D., 1969, Least squares fitting of a straight line with correlated errors: Earth and Planetary Science Letters, v. 5, 320-344 p.

Appendix A: $^{40}Ar/^{39}Ar$ age spectrum, K/Ca and % Radiogenic yields for each sample.

01-CB-001A/#12/DD78

groundmass concentrate

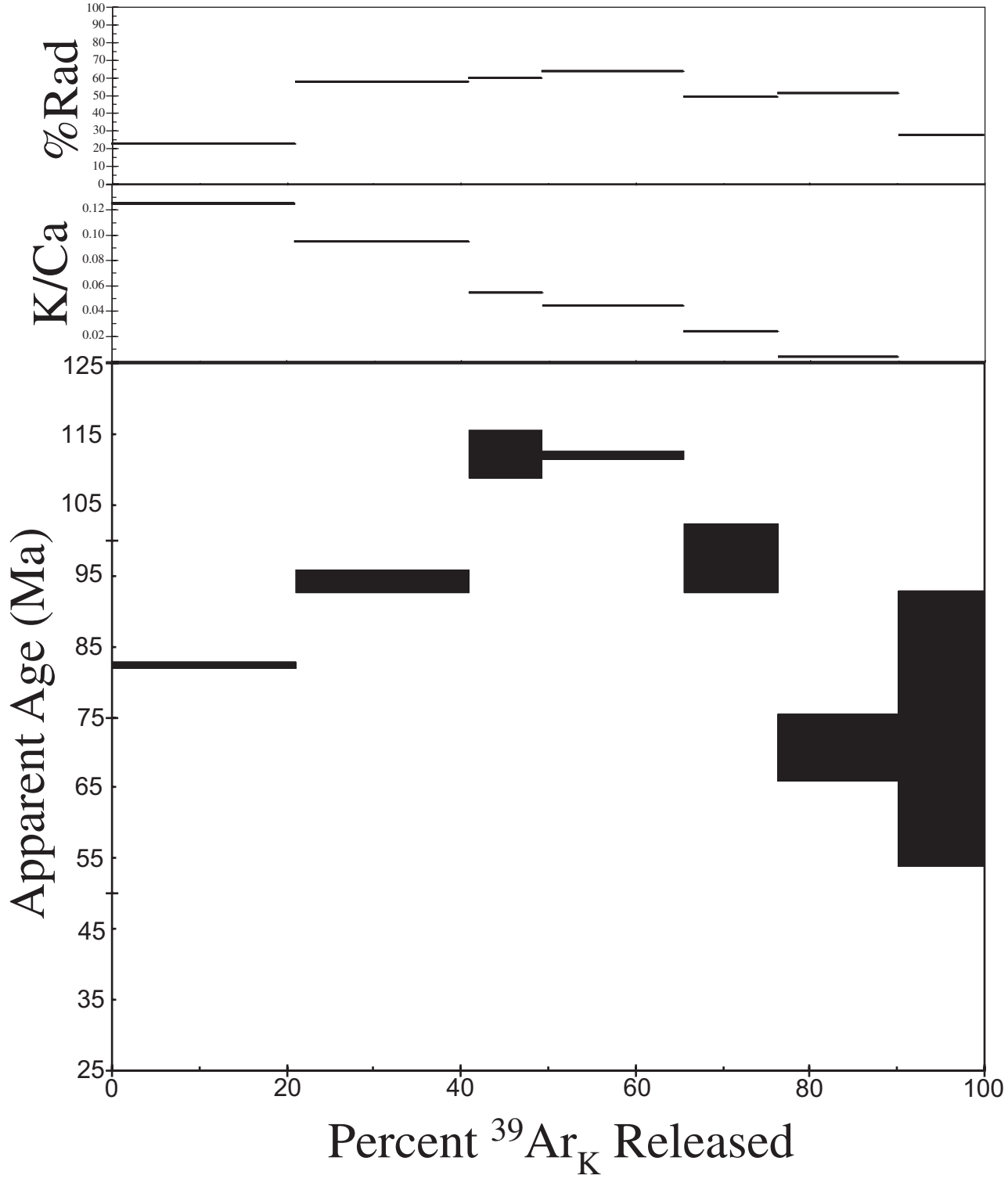

01-CB-002/#11/DD78

groundmass concentrate

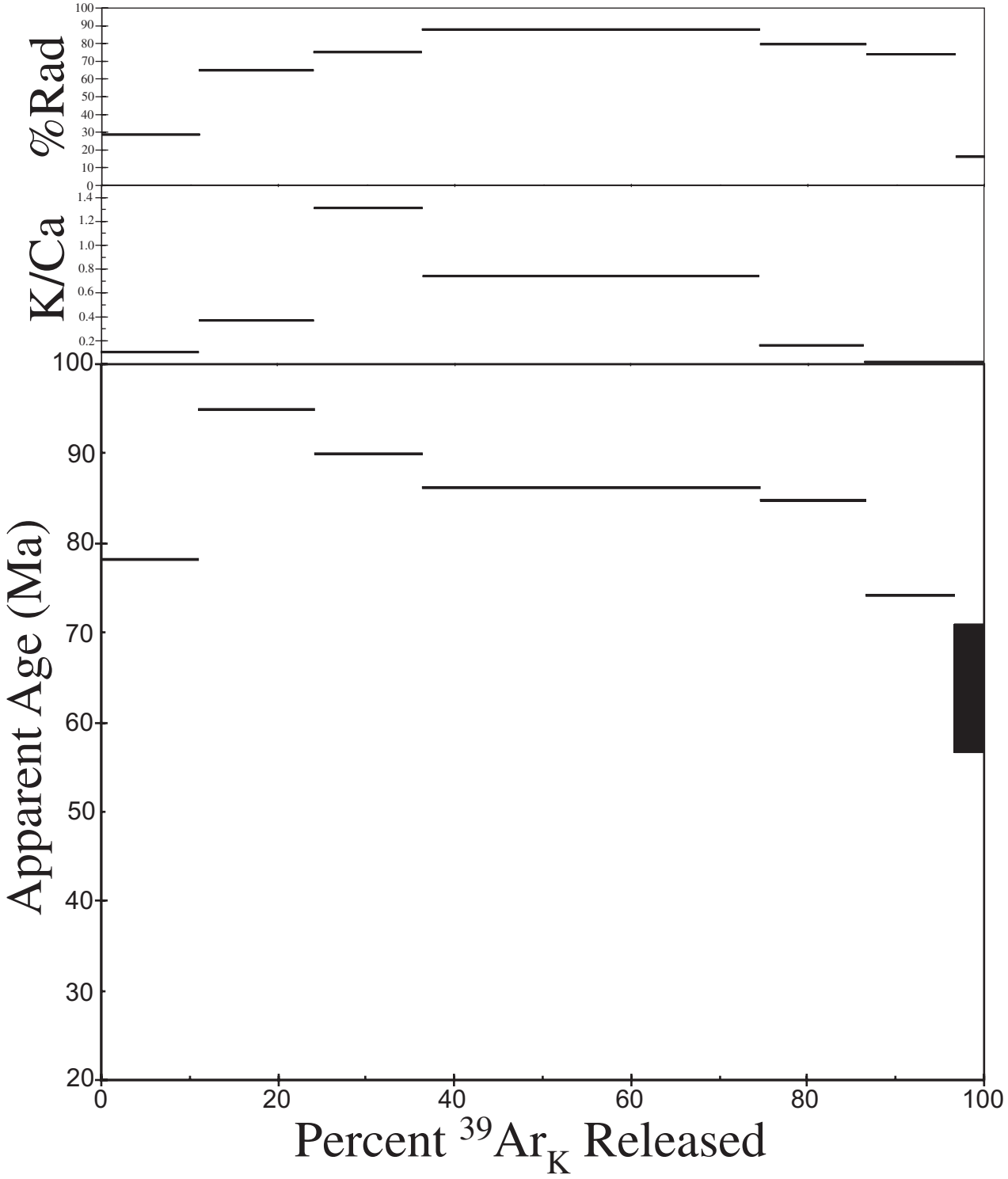

01-CB-002/#8/DD79

groundmass concentrate

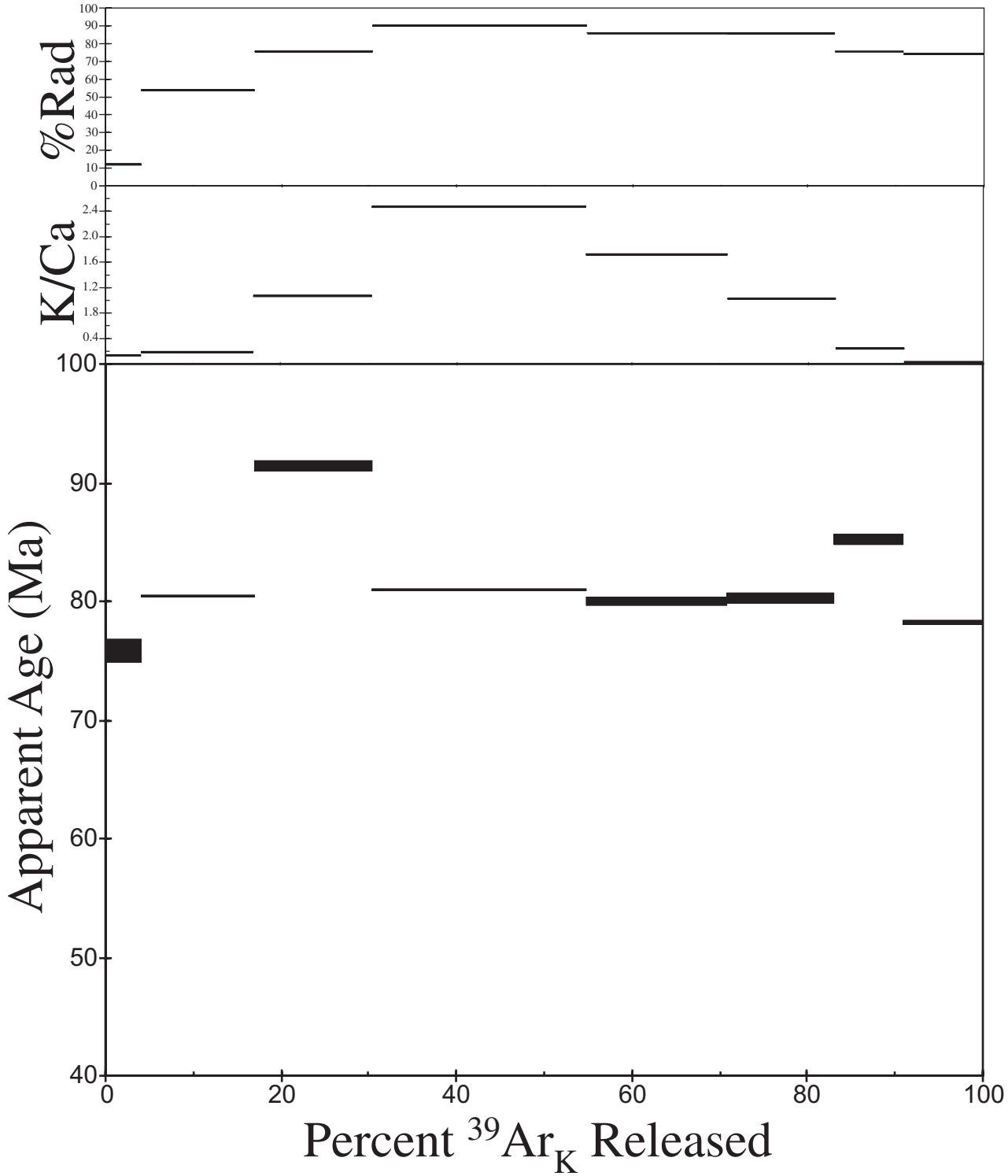

01-CB-005/#1/DD79

K-Feldspar

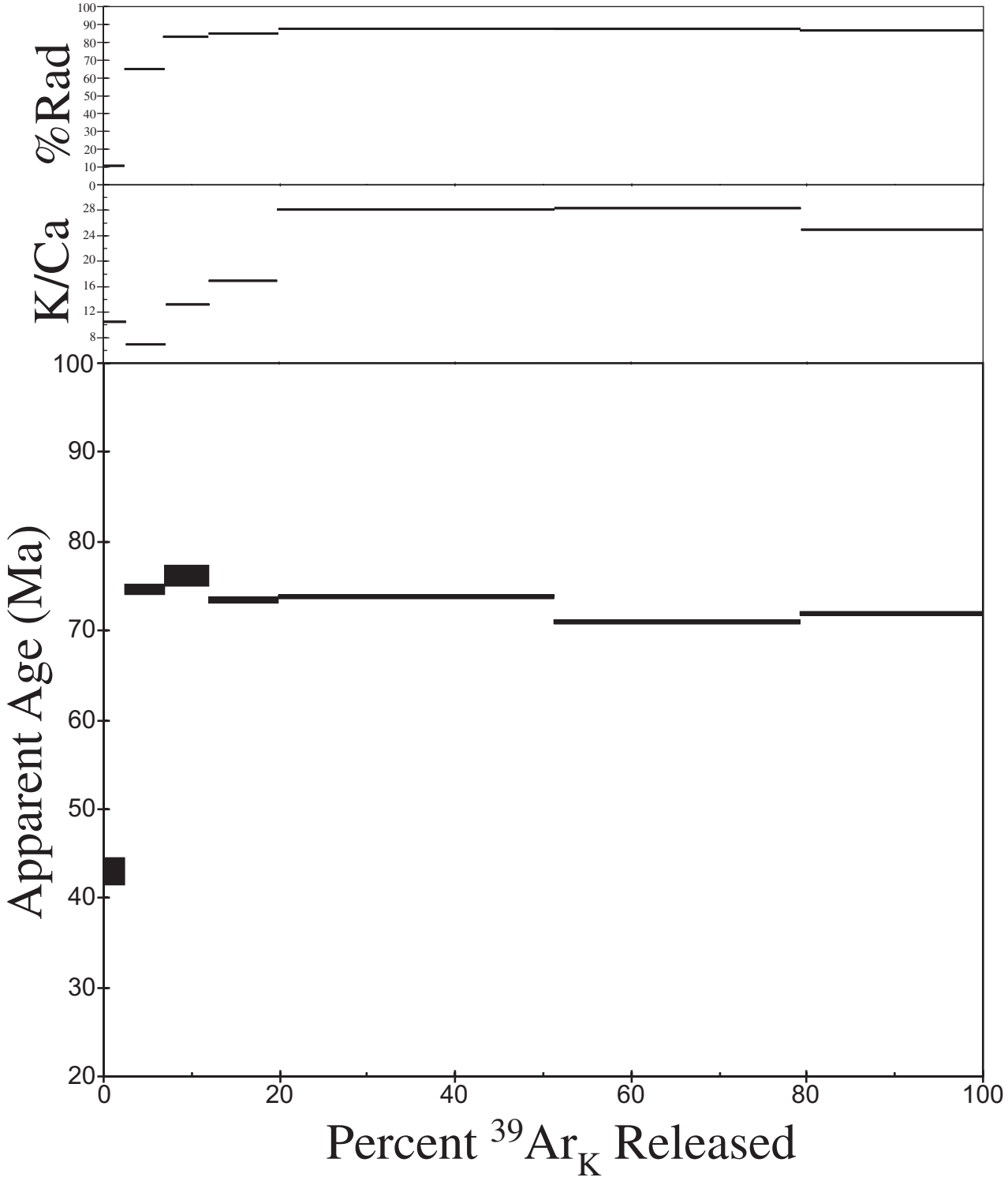

01-CB-005/#3/DD78

K-Feldspar

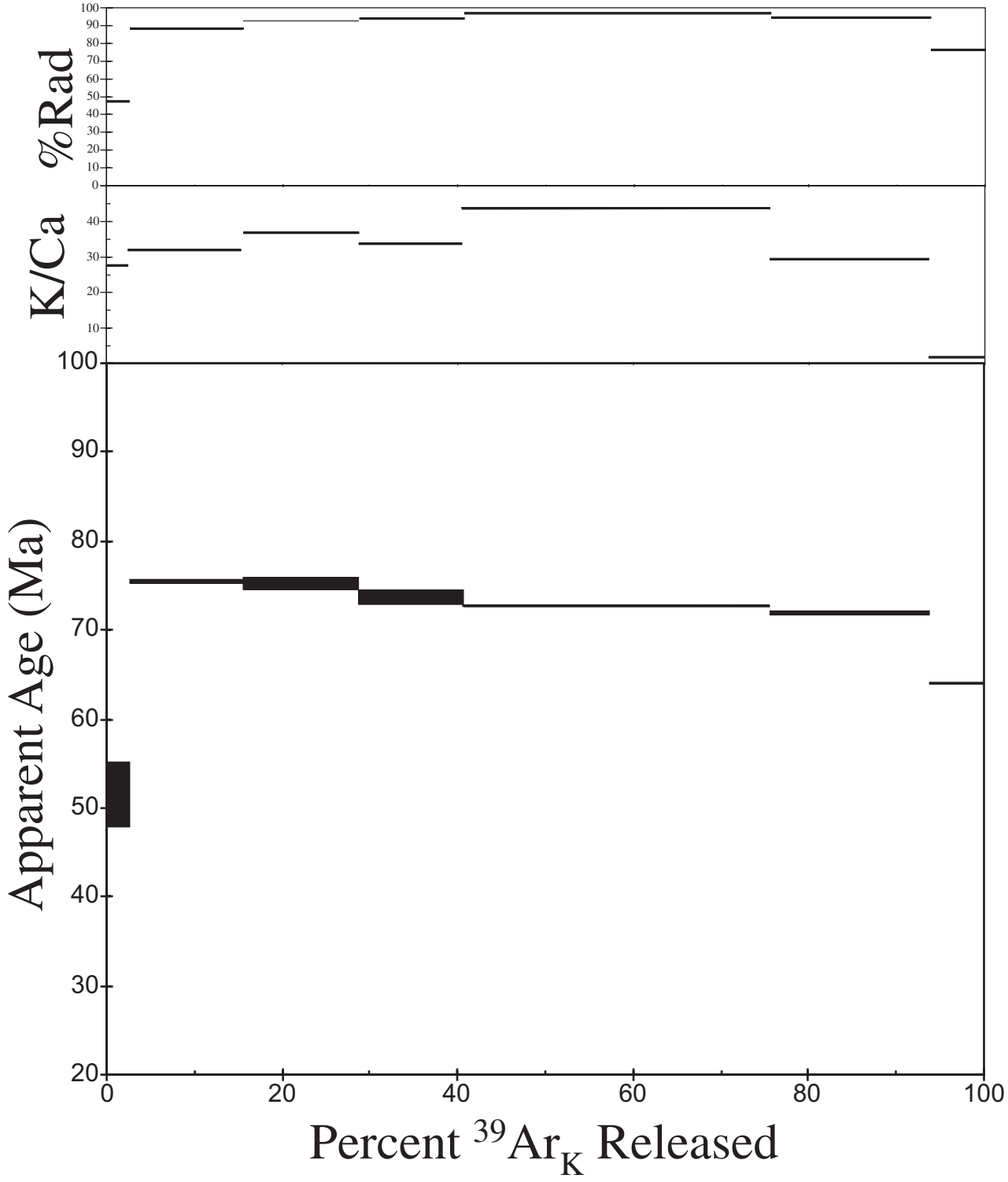

01-CB-006/#2/DD79

K-feldspar

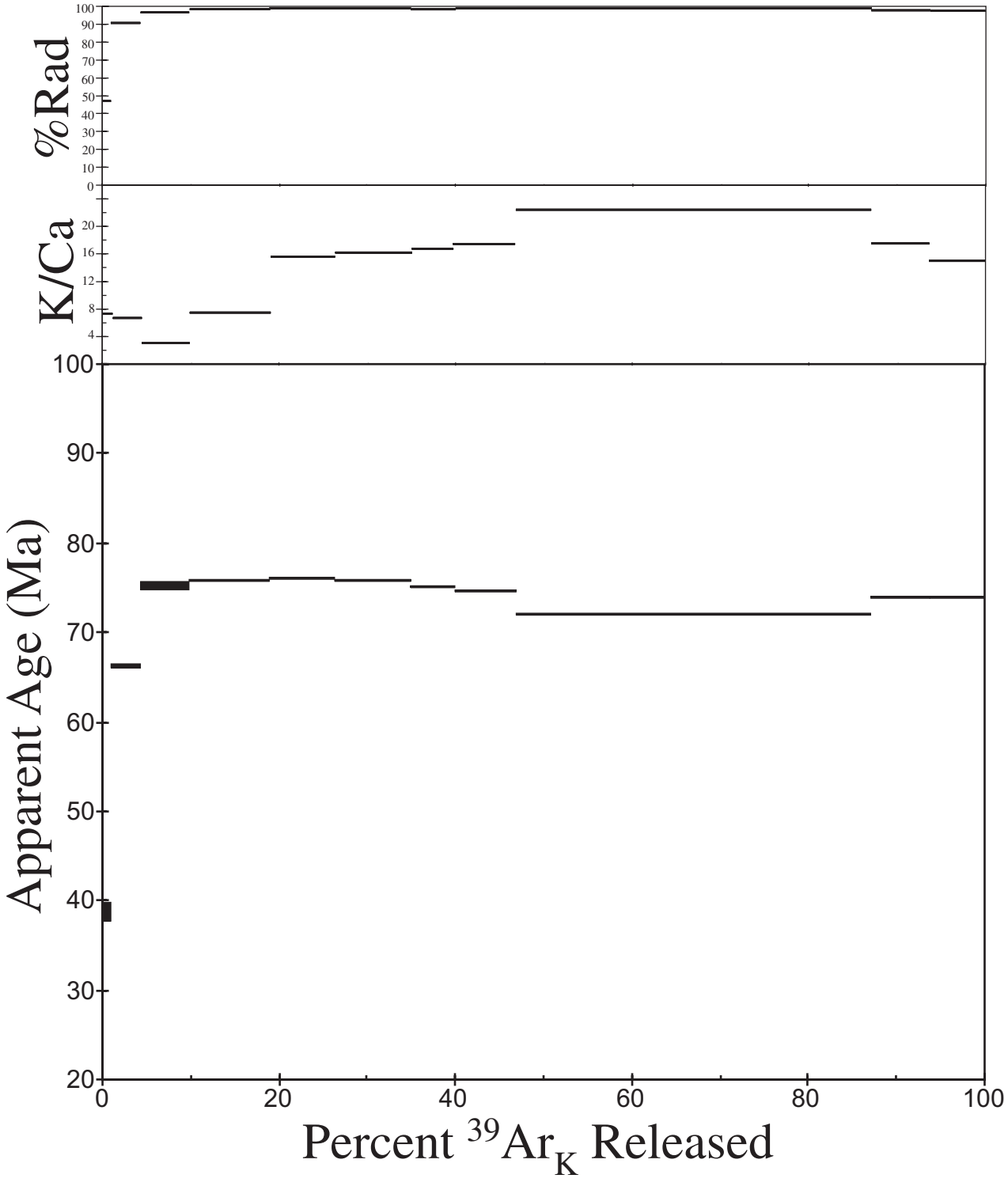

01-CB-007/#7/DD79

groundmass concentrate

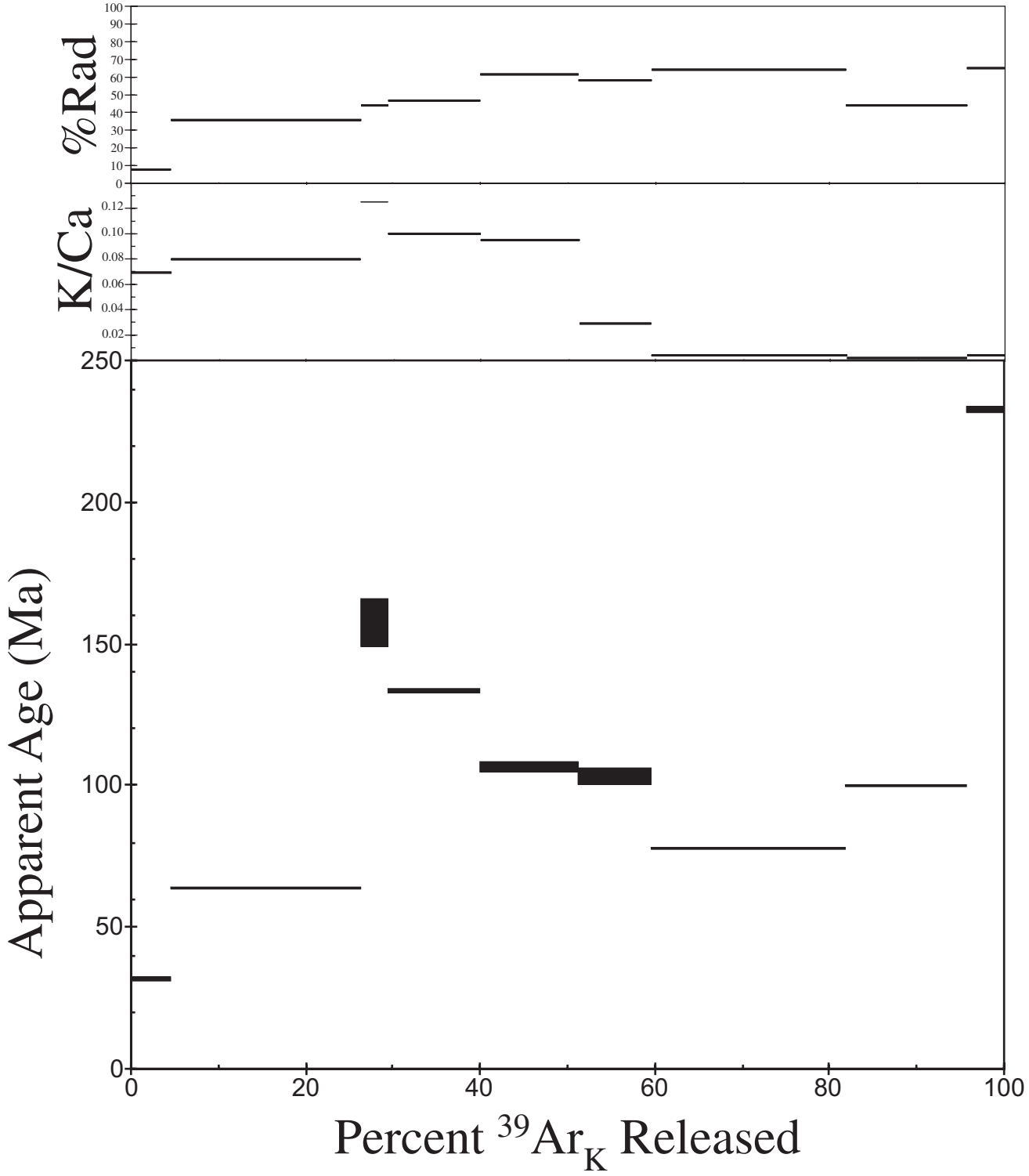

01-CB-008/#14/DD79
Groundmass Concentrate

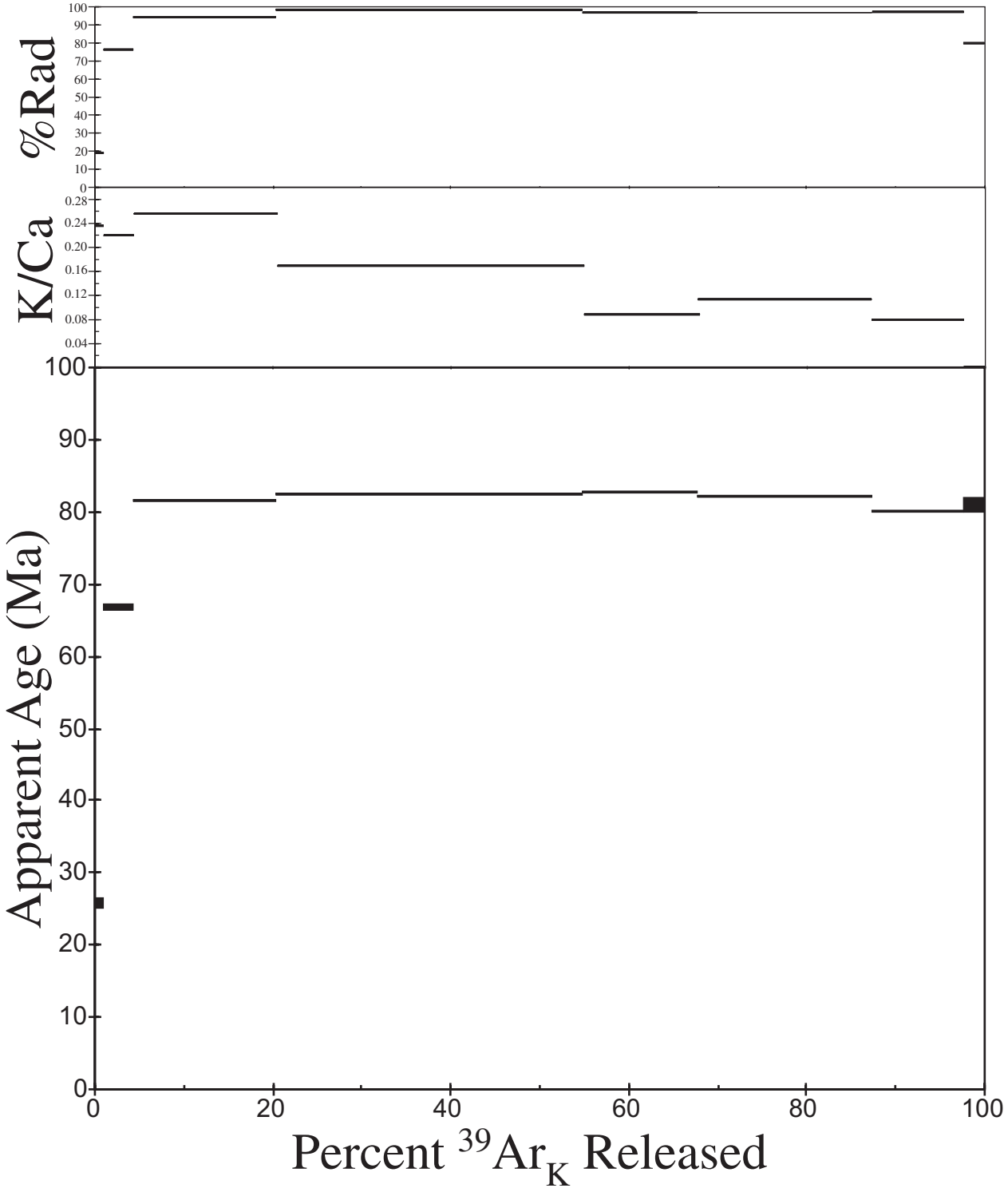

01-CB-008/#4/DD79

Plagioclase

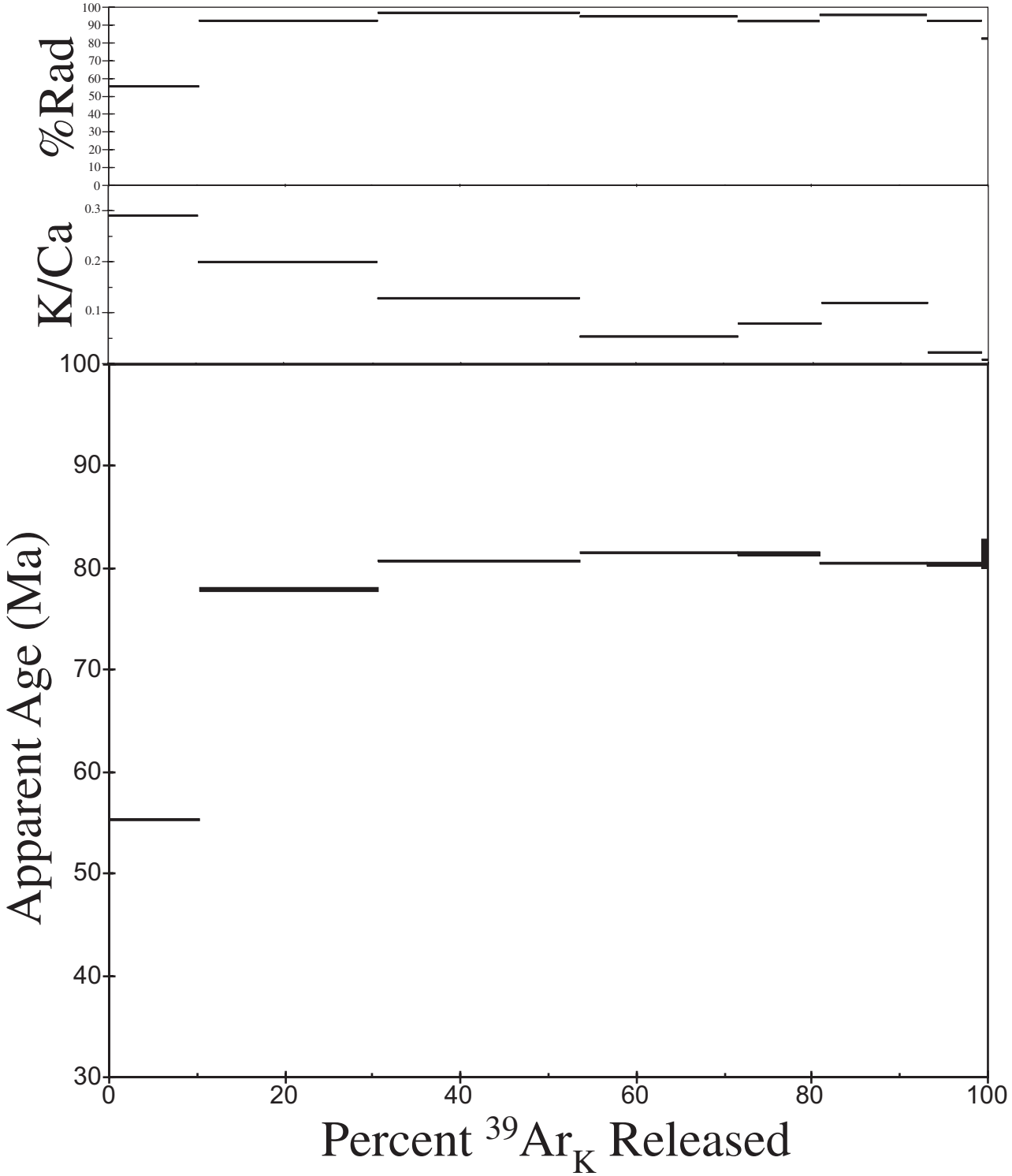

01-CB-009/#109/DD78

Groundmass concentrate

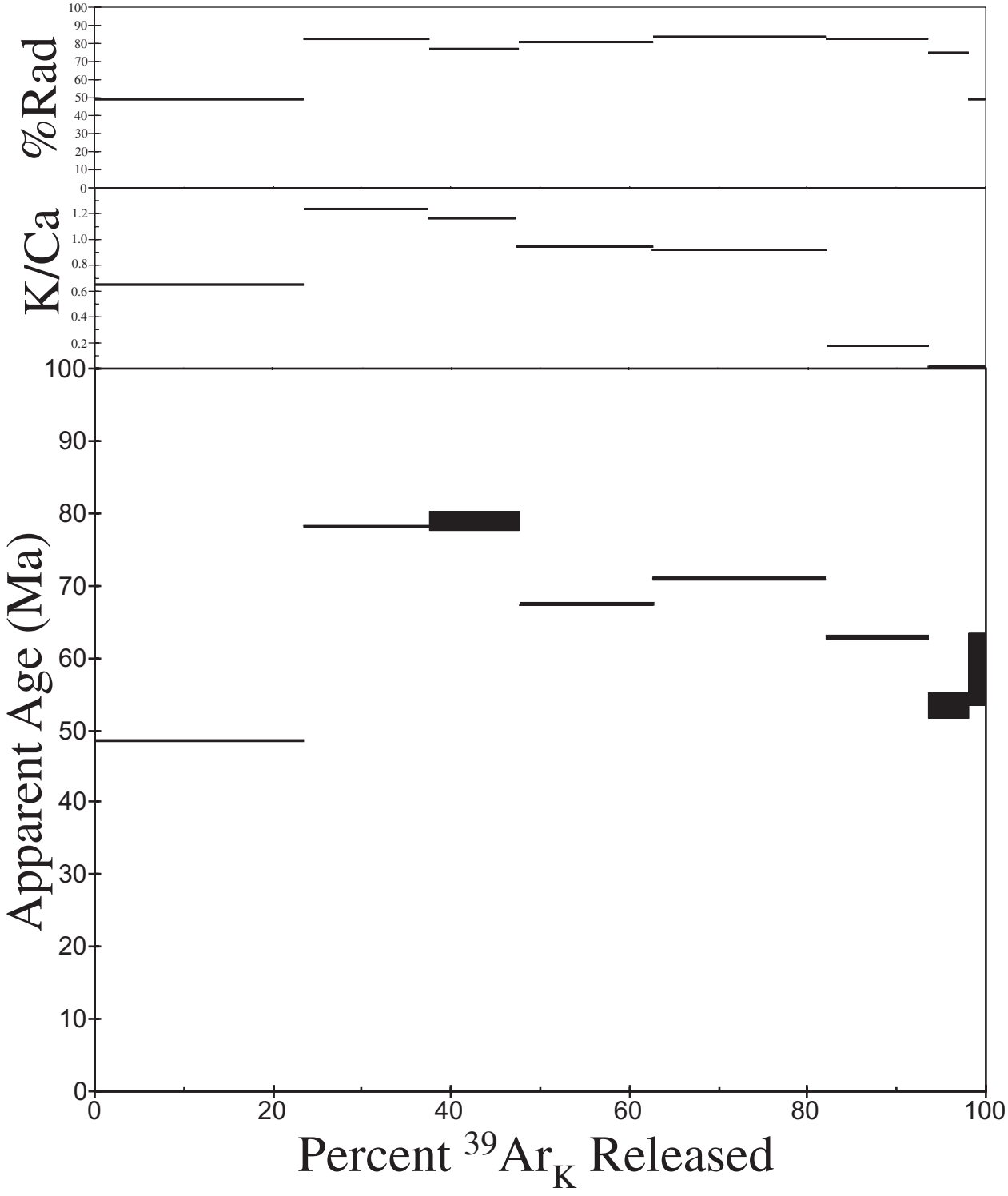

01-CB-010/#6/DD79

Groundmass concentrate

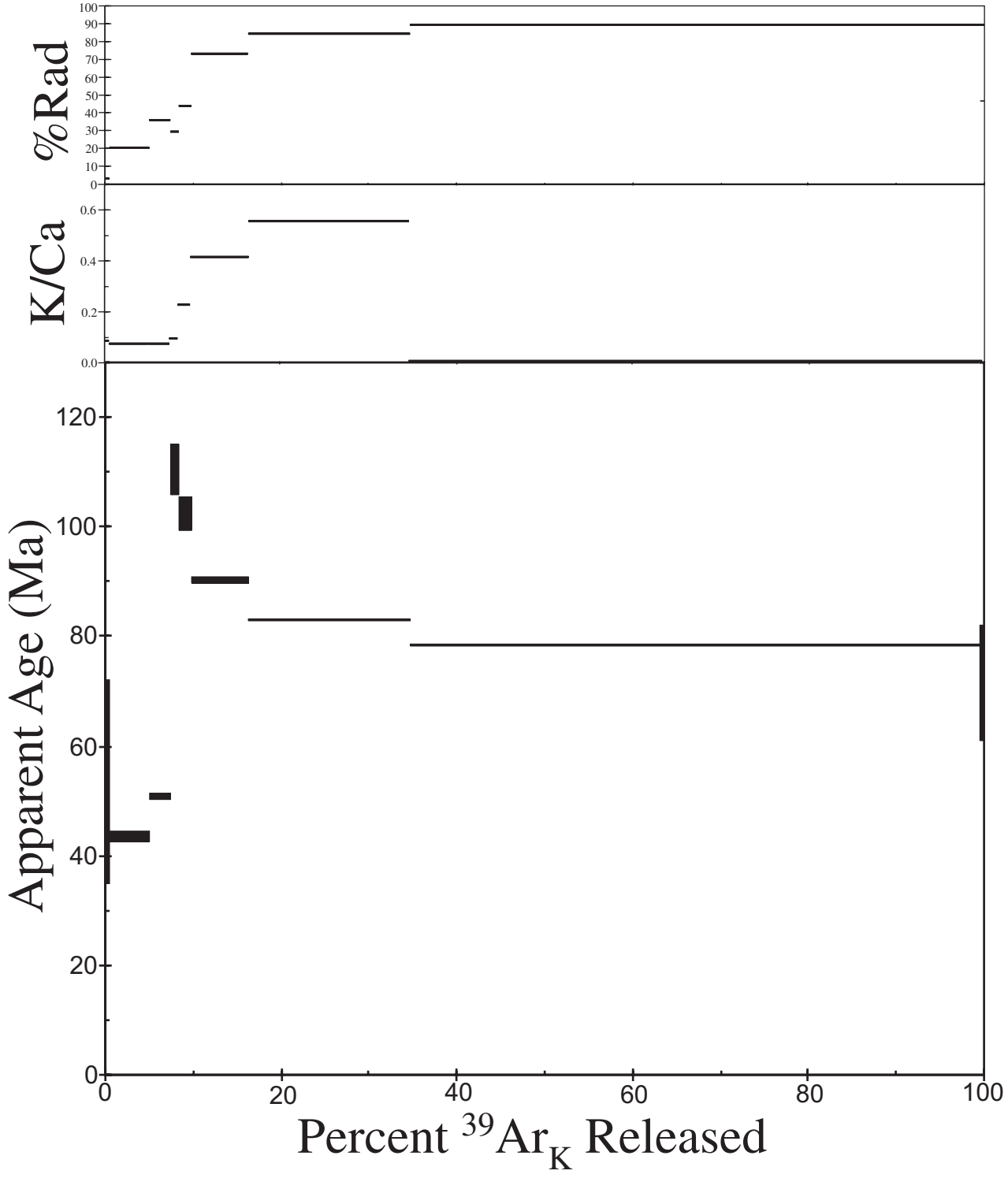

Appendix B: $^{40}Ar/^{39}Ar$ incremental heating data for each sample.

Appendix B. $^{40}Ar/^{39}Ar$ incremental heating data for volcanic intrusions from Uvalde County, Texas.

Temp (°C)	$^{40}Ar_R$[1]	$^{39}Ar_K$	$^{40}Ar_R/^{39}Ar_K$	$^{39}Ar/^{37}Ar$[2]	$\%^{40}Ar_R$	$\%^{39}Ar$	Apparent Age[3] (Ma at ± 1 sigma)
01-CB-001A, #12DD78, Del Rio River Intrusion							
Groundmass Concentrate; .2806g; J-value=.005085±0.1%(1)							
500	0.15794	0.01714	9.215	0.25	23.4	21.1	82.61 ± 0.56
800	0.17112	0.1621	10.554	0.19	58	19.9	94.3 ± 1.5
900	0.08623	0.00684	12.598	0.11	60	8.4	112.0 ± 3.3
1000	0.16485	0.01311	12.571	0.09	63.9	16.1	111.78 ± 0.61
1100	0.09578	0.00878	10.905	0.05	49.5	10.8	97 ± 5
1200	0.08942	0.01132	7.898	0.01	51.7	13.9	71 ± 5
1350	0.06467	0.00788	8.208	0	28.3	9.7	74 ± 19
Total gas age: 91.31±4.35 Ma							
01-CB-002, #11DD78, Knippa Quarry Intrusion							
Groundmass Concentrate (82-100 mesh); .1722g; J-value=.005085±0.1%(1)							
500	0.29237	0.03617	8.083	0.23	40.7	11.1	72.66 ± 0.15
700	0.44599	0.04269	10.448	0.75	64.8	13.1	93.38 ± 0.15
800	0.39042	0.04007	9.744	2.62	72.5	12.3	87.24 ± 0.13
1000	1.14557	0.12415	9.227	1.49	81.3	38.1	82.75 ± 0.14
1100	0.34951	0.03874	9.021	0.34	75.6	11.9	80.91 ± 0.17
1200	0.24766	0.03292	7.523	0.02	71.6	10.1	67.72 ± 0.10
1350	0.06802	0.0112	6.075	0	31.8	3.4	55 ± 9
Total gas age: 80.89±0.56 Ma							
Isochron age (steps 1-7): 76±7 Ma; (40Ar/36Ar)i=241±39							
01-CB-002, #8DD79, Knippa Quarry Intrusion							
Groundmass Concentrate (46-60 mesh); .2438g; J-value=.0105±0.1%(1)							
650	0.19579	0.04779	4.097	0.31	30.3	4.1	75.99 ± 0.97
750	0.64791	0.14923	4.342	0.41	63.1	12.8	80.42 ± 0.12
850	0.77916	0.15743	4.949	2.16	80.5	13.5	91.39 ± 0.47
950	1.24042	0.28353	4.375	4.92	91.5	24.3	81.02 ± 0.12
1050	0.81858	0.18935	4.323	3.44	88.8	16.2	80.09 ± 0.29
1150	0.61907	0.14273	4.337	2.08	88.2	12.2	80.34 ± 0.45
1250	0.42218	0.0917	4.604	0.52	79.6	7.9	85.16 ± 0.43
1400	0.43965	0.10404	4.226	0.1	79.3	8.9	78.32 ± 0.17
Total gas age: 81.99±0.29 Ma.							
Average age (steps 4-6) 80.48±0.29 Ma; Isochron age (steps 1-8): 82.7±2 Ma; (40Ar/36Ar)i=287±16							
01-CB-005, #3DD78, Fort Inge Intrusion							
K-feldspar; .0064g; J-value=.005095±0.1%(1)							
650	0.05111	0.00894	5.718	54.73	47.5	2.6	51.8 ± 3.6
850	0.37597	0.04482	8.388	62.81	87.9	13	75.49 ± 0.27
950	0.38245	0.04568	8.373	73.46	92.4	13.2	75.36 ± 0.70
1050	0.33549	0.04092	8.199	67.33	93.5	11.8	73.83 ± 0.83
1200	0.97607	0.12087	8.075	87.08	96.5	35	72.74 ± 0.11
1350	0.50003	0.06251	7.999	59.03	94.2	18.1	72.07 ± 0.19
1450	0.15383	0.02162	7.115	4.51	76.5	6.3	64.24 ± 0.11
Total gas age: 72.38±0.41 Ma.							
Average age (steps 5-6) 72.41±0.15 Ma; Isochron age (steps 2-6): 71.5±1.1 Ma; (40Ar/36Ar)i=423±57							

Appendix B continued

Temp (°C)	$^{40}Ar_R$[1]	$^{39}Ar_K$	$^{40}Ar_R/^{39}Ar_K$	$^{39}Ar/^{37}Ar$[2]	$\%^{40}Ar_R$	$\%^{39}Ar$	Apparent Age[3] (Ma at ± 1 sigma)
01-CB-005, #1DD79, Fort Inge Intrusion							
K-feldspar; .0102g; J-value=.010504±0.1%(1)							
650	0.07715	0.03323	2.322	21.24	12.6	2.5	43.5 ± 1.5
850	0.23548	0.05843	4.03	14.25	71.5	4.5	74.80 ± 0.61
950	0.2632	0.06408	4.107	26.65	90.9	4.9	76.2 ± 1.1
1050	0.40735	0.10285	3.96	34.03	93.1	7.9	73.53 ± 0.41
1200	1.63445	0.41104	3.976	56.07	95.9	31.5	73.82 ± 0.21
1300	1.39105	0.36365	3.825	56.52	96	27.9	71.07 ± 0.21
1450	1.04681	0.27021	3.874	49.91	95	20.7	71.96 ± 0.20
Total gas age: 72.04±0.33 Ma.							
Average age (steps 4-7) 72.60±0.26 Ma; Isochron age (steps 1-7): 74.1±1.0 Ma; (40Ar/36Ar)i=268±8							
01-CB-006, #2DD79, Intrusion on Highway 90 west of Sabinal							
K-feldspar; .0596g; J-value=.010487±0.1%(1)							
650	0.16164	0.07702	2.099	14.9	47.3	1.1	39.3 ± 1.1
750	0.80127	0.22406	3.576	13.62	90.4	3.3	66.42 ± 0.24
850	1.52209	0.37451	4.064	6.54	96.1	5.5	75.30 ± 0.49
950	2.56789	0.62748	4.092	15.17	97.9	9.1	75.81 ± 0.22
1000	2.0881	0.50851	4.106	31.17	98.4	7.4	76.06 ± 0.12
1050	2.41534	0.58959	4.097	32.48	98.6	8.6	75.88 ± 0.23
1100	1.37299	0.33823	4.059	33.45	97.9	4.9	75.21 ± 0.12
1150	1.92512	0.47828	4.025	34.76	98.1	7	74.59 ± 0.12
1200	10.77533	2.76641	3.895	44.67	98.6	40.3	72.22 ± 0.14
1300	1.79115	0.44904	3.989	35.05	97.4	6.5	73.93 ± 0.11
1400	1.74096	0.43605	3.993	29.98	97.1	6.3	74.00 ± 0.14
Total gas age: 73.30±0.19 Ma.							
Average age (steps 9-11) 73.39±0.13 Ma; Isochron age (steps 1-11): 74.6±1.2 Ma; (40Ar/36Ar)i=336±226							
01-CB-007, #7DD79, Intrusion southeast of Uvalde							
Groundmass Concentrate; .2471g; J-value=.010095±0.1%(1)							
650	0.01327	0.00712	1.863	0.14	8.4	4.5	33.61 ± 0.66
750	0.12742	0.03477	3.665	0.16	36.3	21.8	65.54 ± 0.47
850	0.04454	0.00492	9.052	0.25	44.2	3.1	158 ± 8
950	0.12969	0.01695	7.651	0.2	46.9	10.6	134.2 ± 0.98
1050	0.10868	0.01785	6.089	0.19	61.4	11.2	108 ± 1.8
1150	0.07936	0.01345	5.899	0.06	58.4	8.4	104 ± 3
1250	0.15684	0.03529	4.444	0.01	64.1	22.2	79.17 ± 0.56
1350	0.12626	0.0221	5.713	0	44.2	13.9	101.2 ± 0.15
1450	0.0919	0.00676	13.593	0.01	65.1	4.2	232 ± 1.00
Total gas age: 97.73±1.07 Ma.							
Maximum possible age (steps 7) 79.2±0.6 Ma; Isochron age (steps 1-9): 105±27 Ma; (40Ar/36Ar)i=287±67							

Appendix B continued

Temp (°C)	$^{40}Ar_R$[1]	$^{39}Ar_K$	$^{40}Ar_R/^{39}Ar_K$	$^{39}Ar/^{37}Ar$[2]	$\%^{40}Ar_R$	$\%^{39}Ar$	Apparent Age[3] (Ma at ± 1 sigma)
01-CB-008, #4DD79, Intrusion north of Cline							
Plagioclase; .250g; J-value=.010282±0.1%(1)							
650	1.07178	0.35171	3.047	0.58	55.8	10.2	55.66 ± 0.09
800	3.01013	0.70078	4.295	0.4	92.1	20.4	77.97 ± 0.27
900	3.5217	0.79144	4.45	0.26	96.6	23	80.70 ± 0.12
1000	2.78118	0.61814	4.499	0.11	94.4	18	81.58 ± 0.12
1100	1.4454	0.32189	1.49	0.16	91.9	9.4	81.42 ± 0.26
1200	1.84801	0.4162	1.44	0.24	95.4	12.1	80.53 ± 0.12
1300	0.92759	0.20933	4.431	0.05	92.1	6.1	80.38 ± 0.18
1400	0.11485	0.02556	4.494	0.02	82.1	0.7	81.5 ± 1.4
Total gas age: 77.79±0.17 Ma.							
Average age (steps 3-7) 80.92±0.16 Ma; Isochron age (steps 2-8): 80.36±0.91 Ma; (40Ar/36Ar)i=300±33							
01-CB-008, #14DD79, Intrusion north of Cline							
Groundmass concentrate; .1722g; J-value=.009845±0.1%(1)							
650	0.03491	0.02336	1.494	0.47	19.4	1	26.35 ± 0.62
750	0.31121	0.08122	3.832	0.44	76.2	3.3	66.80 ± 0.41
850	1.83919	0.39138	4.699	0.51	93.9	16.1	81.59 ± 0.15
950	3.98219	0.83885	4.747	0.34	97.9	34.4	82.40 ± 0.13
1050	1.51506	0.3176	4.77	0.18	96.5	13	82.79 ± 0.13
1150	2.24887	0.4754	4.73	0.23	96.6	19.5	82.12 ± 0.13
1250	1.16106	0.25182	4.611	0.16	96.7	10.3	80.08 ± 0.12
1400	0.26521	0.05689	4.662	0.01	79.6	2.3	81.0 ± 1
Total gas age: 80.95±0.17 Ma.							
Highest point in spectrum (step 5) 82.79±0.13 Ma; Isochron age (steps 3-6, and 8): 82.68±0.24 Ma; (40Ar/36Ar)i=252±7							
01-CB-009, #109DD78, Intrusion west of Uvalde on highway 90							
Groundmass concentrate; .2628g; J-value=.005045±0.1%(1)							
500	0.75588	0.13924	5.429	1.31	49.4	23.4	48.74 ± 0.08
700	0.73653	0.08397	8.771	2.46	82.2	14.1	78.11 ± 0.12
800	0.52703	0.05949	8.858	2.33	76.8	10	78.9 ± 1.4
900	0.67564	0.08965	7.536	1.89	80.6	15.1	67.32 ± 0.10
1000	0.92449	0.1165	7.935	1.84	83.4	19.6	70.81 ± 0.11
1100	0.47518	0.06742	7.048	0.37	82.6	11.3	63.03 ± 0.28
1200	0.1667	0.02789	5.977	0.01	74.7	4.7	53.6 ± 1.8
1350	0.07134	0.01088	6.556	0	49.4	1.8	58.70 ± 4.92
Total gas age: 65.08±0.41 Ma.							
Highest point in spectrum (step 3) 78.9±1.4 Ma; Isochron age (steps 1-8): 74±7 Ma; (40Ar/36Ar)i=188±7							

Appendix B continued

Temp (°C)	$^{40}Ar_R$[1]	$^{39}Ar_K$	$^{40}Ar_R/^{39}Ar_K$	$^{39}Ar/^{37}Ar$[2]	$\%^{40}Ar_R$	$\%^{39}Ar$	Apparent Age[3] (Ma at ± 1 sigma)
01-CB-010, #6DD79, Intrusion south of Sabinal							
Groundmass concentrate; .2868g; J-value=.010382±0.1%(1)							
600	0.01196	0.00409	2.926	0.18	3.7	0.4	54 ± 18
700	0.12753	0.0534	2.388	0.16	20.9	4.7	44.18 ± 0.77
800	0.07376	0.02655	2.778	0.16	36.6	2.3	51.30 ± 0.54
900	0.073	0.01202	6.071	0.2	29.9	1	110.3 ± 4.4
1000	0.09333	0.0166	5.622	0.46	44.2	1.4	102.3 ± 3.1
1100	0.37774	0.07614	4.961	0.83	73.1	6.6	90.60 ± 0.60
1250	0.95685	0.21032	4.55	1.11	84.2	18.3	83.26 ± 0.16
1400	3.19008	0.74446	4.285	0.02	89.1	64.9	78.52 ± 0.12
1500	0.01163	0.00297	3.914	0.01	46.9	0.3	72 ± 10

Total gas age: 78.57±0.40 Ma.

Maximum age (Step #3), 78.52±0.12 Ma; Isochron age (steps 1-9): 80±7 Ma; (40Ar/36Ar)i=281±23

Note. These are abbreviated footnotes for Appendix B.

1. **Radiogenic $^{40}Ar(^{40}Ar_R)$ is the total ^{40}Ar derived from natural radioactive decay of ^{40}K after all corrections from non-derived ^{40}Ar, including atmospheric ^{40}Ar and reactor-produced ^{40}Ar, have been made. K-derived ^{39}Ar ($^{39}Ar_K$) is the total ^{39}Ar derived from the epithermal neutron-induced $^{39}K(n,p)^{39}Ar$ after corrections for non-^{39}Ar-derived ^{39}Ar, including ^{42}Ca-derived ^{39}Ar, are made. F is the quantity resulting from the division of radiogenic ^{40}Ar and K-derived ^{39}Ar. Quantities for radiogenic ^{40}Ar and K-derived ^{39}Ar are given in volts of signal measured on a Faraday detector by a digital voltmeter. These quantities can be converted to moles, using the mass spectrometer sensitivity at the time of measurement of $9.736x10^{-13}$ moles of argon per volt of signal. The measured $^{40}Ar/^{36}Ar$ ratio used for mass discrimination correction is 298.9.**
2. **By multiplying the $^{39}Ar/^{37}Ar$ ratios by 0.5, the relative approximate K/Ca distribution of the samples may be obtained.**
3. **Error estimates for apparent ages of individual temperature steps were assigned by using the equations of Dalrymple and others (1981); however, the equations were modified to allow the option of choosing the larger of separately derived errors in the F-value-either a calculated error or an experimental error determined from the reproducibility of identical samples.**